



Nitrogen Cycling in CMIP6 Land Surface Models: Progress and Limitations

Taraka Davies-Barnard^{1,2}, Johannes Meyerholt², Sönke Zaehle², Pierre Friedlingstein^{1,3}, Victor Brovkin⁴, Yuanchao Fan^{5,6}, Rosie A. Fisher^{7,8}, Chris D. Jones⁹, Hanna Lee⁵, Daniele Peano¹⁰, Benjamin Smith^{11,12}, David Wårlind^{11,12}, and Andy Wiltshire⁹

¹University of Exeter, Exeter, UK

²Max Planck Institute for Biogeochemistry, Jena, Germany

³Laboratoire de Meteorologie Dynamique, Institut Pierre-Simon Laplace, CNRS-ENS-UPMC-X, Departement de Geosciences, Ecole Normale Supérieure, 24 rue Lhomond, 75005 Paris, France

10 ⁴Max Planck Institute for Meteorology, Hamburg, Germany

⁵NORCE Norwegian Research Centre, Bjerknes Centre for Climate Research, Bergen, Norway

⁶Harvard University, Cambridge, USA

⁷National Center for Atmospheric Research, Boulder, Colorado, USA

15 ⁸Centre Européen de Recherche et de Formation Avancée en Calcul Scientifique, Toulouse, France

⁹Met Office Hadley Centre, Exeter, UK

¹⁰Fondazione Centro euro-Mediterraneo sui Cambiamenti Climatici, Bologna, Italy

¹¹Department of Physical Geography and Ecosystem Science, Lund University, Lund, Sweden

¹²Hawkesbury Institute for the Environment, Western Sydney University, Richmond, Australia

20 *Correspondence to:* T. Davies-Barnard (t.davies-barnard@exeter.ac.uk)

Abstract. The nitrogen cycle and its effect on carbon uptake in the terrestrial biosphere is a recent progression in earth system models. As with any new component of a model, it is important to understand the behaviour, strengths, and limitations of the various process representations. Here we assess and compare five models with nitrogen cycles that will be used as the terrestrial components of some of the earth system models in CMIP6. We use a historical control simulation and two perturbations to assess the models' nitrogen-related performance: a simulation with atmospheric carbon dioxide 200 ppm higher, and one with nitrogen deposition increased by 50 kg N ha⁻¹ yr⁻¹. We find that, despite differing nitrogen cycle representations, all models simulate recent global trends in terrestrial productivity and net carbon uptake commensurate with observations. The between-model variation is likely more influenced by other, non-nitrogen parts of the models. Globally, the productivity response to increased carbon dioxide is commensurate with observations for four of the five models, but highly spatially variable within and between models. The productivity response to increased nitrogen is significantly lower than observed in two of the five models. The global and tropical values are generally better represented than boreal, tundra, or other high latitude areas. These results are due to divergent though valid choices in the representation of key processes. They show the need for better understanding and more provision of observational constraints of nitrogen processes, especially nitrogen-use efficiency and biological nitrogen fixation.

35



1 Introduction

The terrestrial carbon (C) cycle currently removes around a third of anthropogenic carbon emissions from the atmosphere (Friedlingstein et al., 2019; Le Quéré et al., 2018). Changes in this uptake will affect the allowable emissions for targets such as limiting warming to 1.5°C (Millar et al., 2017; Müller et al., 2016). Nitrogen (N) is required to synthesise new plant tissue (biomass) out of plant-assimilated carbon, in differing ratios across biomes and tissue types (McGroddy et al., 2004). Therefore, future projections of terrestrial carbon uptake and allowable emissions are dependent on N availability, particularly under high atmospheric carbon dioxide (CO₂) conditions (Arora et al., 2019; Wieder et al., 2015b; Zaehle et al., 2014b). Earth System Models (ESMs) are tools to project the responses of the coupled earth system and its components such as the atmosphere, biosphere, and oceans to anthropogenic and natural forcings (Anav et al., 2013; Arora et al., 2013; Friedlingstein et al., 2006; Jones et al., 2013). The Fifth Phase of the Coupled Model Intercomparison Project (CMIP5, Taylor et al., 2012) had numerous models with a global C cycle but only two with terrestrial N cycling (Thornton et al., 2009). However, predictions of terrestrial C storage would decrease by 37 – 58% if ESMs accounted for the constraints on terrestrial C sequestration imposed by the tight coupling of the C cycle with the N cycle (Wieder et al., 2015b; Zaehle et al., 2014b).

50

The latest generation of models in CMIP6 (Eyring et al., 2016) have at least six models that incorporate the N cycle (Arora et al., 2019). These models employ a range of assumptions and process formulations, reflecting divergent theory and significant knowledge gaps (Zaehle and Dalmonech, 2011). Since variation in N is a main source of uncertainty for the carbon cycle (Song et al., 2019), assessment of the models' N cycle processes is required to understand the headline performance and sensitivity of the N cycle to changes in atmospheric CO₂ and N inputs. In this study, we evaluate land surface models (LSMs) with N cycles employed in the latest generation of European ESMs that contribute to CMIP6. We use a range of upscaled field-based observations, satellite observations, and model-to-model comparisons to assess the behaviour and performance of the models. The approach of assessing ESM N cycles via their corresponding offline LSMs, driven by a standardised set of model forcing, has the advantage of making model projections directly comparable while giving a representative view of the latest N cycle developments.

60

2 Methods

2.1 Models

We use five LSMs that are the land components of five European ESMs taking part in CMIP6. The models employ a diverse set of process representations of the N cycle and its coupling to the C cycle. The key N process formulations are summarized in Table 1. A brief description of each model follows.

65



The Community Land Model version 4.5 (CLM4.5; Koven et al., 2013; Oleson et al., 2010) is used in the Euro-Mediterranean Centre on Climate Change coupled climate model (CMCC-CM2; Cherchi et al., 2019). The N component is described in Koven et al., (2013). CLM4 was the first N model for ESMs, used in CMIP5. The N cycling component of CLM4.5 is similar to CLM4, but other features of the model, such as leaf physiological traits (Bonan et al., 2012), were modified.

The Community Land Model version 5 (CLM5; Lawrence et al., 2020) is used in the Norwegian Earth System Model version 2 (NorESM2). CLM5 is the latest version of CLM and represents a suite of developments on top of CLM4.5. CLM5 prescribes crop management including nitrogen fertilizer use and irrigation fraction at annual time step. The N component is described in Fisher et al., (2010); and Shi et al., (2016). The key difference for the N cycle is the implementation of a C cost basis for acquiring N, derived from the Fixation and Uptake of Nitrogen (FUN) approach (Fisher et al., 2010).

The JSBACH version 3.20 model (Goll et al., 2017) is used in the Max Planck Earth System Model version 1.2 (MPI-ESM; Mauritsen et al., 2019).

The Joint UK Land Environment Simulator version 5.4 (JULES; Best et al., 2011; Clark et al., 2011) is used in the UK Earth System Model (UKESM1; Sellar et al., 2020.). The N component is described in Wiltshire et al. (forthcoming) and Sellar et al., (2020).

The Lund-Potsdam-Jena General Ecosystem Simulator version 4.0 (LPJ-GUESS; Olin et al., 2015; Smith et al., 2014) is used in the European community Earth-System Model (EC-Earth; Hazeleger et al., 2012). The N component is described in Smith et al., (2014).

2.2 Forcing Data

All models ran a global spin-up for all ecosystem pools up to the year 1860, forced by a constant atmospheric CO₂ concentration of 287.14 ppm, cycling global climate data at 0.5° x 0.5° resolution for the years 1901-1930 from the CRU-NCEP dataset version 7.0 (New et al., 2000), and assuming constant 1860 land-use from the Hurtt et al., (2011) database. Next, transient runs were performed for the 1861-1900 period with the same climate forcing as the spin-up, but now including varying atmospheric CO₂ concentrations from synthesized ice core and National Oceanic and Atmospheric Administration (NOAA) measurements, as well as annually varying land-use from Hurtt et al., (2011). The simulations were then continued for 1901-2015 under fully dynamic forcing including climate. The N deposition is taken from the Atmospheric Chemistry and Climate Model Intercomparison Project (Lamarque et al., 2013).

The models applied their individual soil spin-ups according to their respective conventions. The goal of the spin-up procedure is to obtain quasi-steady states of the ecosystem pools in relation to climate, avoiding drifting pool sizes due to lack of equilibrium, especially by slow-turnover soil organic matter pools. Because of differences among the models, pool sizes after spin-up are not identical. However, we presume that model responses to perturbations do not depend strongly on the initial model states if those remain within a reasonable range.



2.3 Model Experiments

In addition to the Control run described above, two experiments were run for the period 1996-2015: increased CO₂ (+CO₂) and increased N (+N). These two experimental runs are compared to the corresponding 1996-2015 simulations from the unperturbed Control runs.

For the increased CO₂ experiment (+CO₂) the atmospheric CO₂ concentration was abruptly increased to constant 550 ppm. This is almost twice the pre-industrial atmospheric CO₂ of 280 ppm or a 200 ppm increase compared to the 1996 atmospheric CO₂ of ~350 ppm.

For the increased N experiment (+N) N deposition was abruptly increased by 50 kg N ha⁻¹ yr⁻¹, which is roughly equivalent to typical N fertilisation of crops and around 5 – 10 times higher than typical background N deposition (Zak et al., 2017).

2.4 Analytical Framework

To help generalize the key C-N processes for each model under the +CO₂ and +N scenarios, we use a simple framework that relates N-limited plant growth (NPP) to whole-plant N-use efficiency (NUE; newly constructed biomass C per unit N taken up) and plant N uptake (Zaehle et al., 2014a):

$$NPP = NUE * N_{up} \quad (1)$$

where N_{up} includes plant uptake of soil inorganic N of any origin, i.e. atmospheric deposition, fertilization, decomposition of plant litter, or biological nitrogen fixation (BNF).

This paradigm assumes that ecosystem N input from deposition or fixation enters the soil and then becomes available for plant uptake.

As a consequence of Eq. 1, we consider changes in plant growth induced from perturbations as resulting from changes in NUE or N_{up} :

$$\Delta NPP = \Delta NUE * \Delta N_{up} \quad (2)$$

Our focus is on how models differ in inorganic N availability to plants and plant NUE. If these are constant, changes would be limited to shifts in C allocation between plant organs with different C:N. Flexible C:N within plant organs allows for more complex interactions through changes in internal stoichiometry under perturbation (Meyerholt and Zaehle, 2015).

We also use a simplified N budget to assess the change in N:

$$\Delta N = N_{dep} + BNF - N_{loss} \quad (3)$$



130 Where N_{dep} is the N deposition, BNF is the biological nitrogen fixation, and N_{loss} is the N lost from gaseous and leaching pathways as declared by the models. Note that crop fertilisation is not included here, as it is assumed to remain constant between the 3 simulations.

3 Results

3.1 Control Run Results

135 The N cycle acts primarily as a restriction on the productivity of the C cycle, so theoretically the addition of an N cycle should increase the accuracy of modelled GPP. This generation of N models are generally consistent within observational constraints, showing an improvement compared to CMIP5 N models (Arora et al., 2013; Shao et al., 2013). All the models have global total GPP within the error margin of the estimate based on upscaled flux tower data (MTE) by Jung et al., (2011) and are close to the central estimate (see Fig. 1f). Large areas within all the models are well represented. For key regions, 140 such as the Amazon basin, all models are within ~30% of the observed GPP.

The global scale agreement with total observed GPP obscures considerable regional variability and errors in latitudinal patterns of GPP (SI Fig. 1). Consistent with having the highest global GPP of the models, LPJ-GUESS has widespread higher than observed GPP, particularly in the northern hemisphere outside Western Europe (SI Fig. 2). Combined with lower than observed GPP in parts of the tropics, LPJ-GUESS exhibits a too little latitudinal gradient of GPP. CLM5 also has a 145 reduced gradient trend, though to a lesser extent (SI Fig. 2). JSBACH has the opposite issue, with higher than observed GPP in the parts of the tropics, particularly the Amazonia area of northern South America (Fig. 1 and SI Fig. 2). This gives an overall steeper than observed latitudinal gradient of GPP in JSBACH.

The spatial variability in N limitation (LeBauer and Treseder, 2008; Schulte-Uebbing and Vries, 2018) might suggest that models with an N cycle could represent more N limited areas better. The model errors compared with MTE in GPP is largest 150 in the tropics, which have low N limitation (ibid). However, in the far northern high-latitudes, which are highly N limited (ibid), the model-MTE agreement is also weak (Fig. 1a-e). As a proportion of observed GPP, all the models show either over or underestimations of GPP in tundra and boreal areas of Eurasia and America. All the models except JSBACH have extensive areas of higher than observed GPP in these high-latitude regions. Where the models are overestimating Control run GPP in N limited areas (LeBauer and Treseder, 2008; Schulte-Uebbing and Vries, 2018) suggests the N cycle model may not 155 be correctly simulating key processes that limit growth in these cold and N limited areas.

Despite having some shared components, CLM5 and CLM4.5 show different GPP patterns, particularly in the high latitudes. CLM5 models photosynthesis rates and GPP differently from CLM4.5 due to the implementation of a flexible C:N scheme (versus fixed C:N in CLM4.5) and the Leaf Use of Nitrogen for Assimilation model (LUNA, Xu et al., 2012 and Ali et al., 2016). Other key differences include stomatal conductance in CLM5 (Medlyn et al., 2011) is based on the N-limited net 160 photosynthesis rather than on potential photosynthesis as in CLM4.5. Additionally, GPP can be more affected by non-N cycle aspects of the models, such as the new plant hydraulic stress function (Kennedy et al., 2019) added in CLM5.



The global net ecosystem productivity (NEP), i.e. the net balance of C assimilation through photosynthesis and C losses to heterotrophic and autotrophic respiration as well as land use changes is calculated via annual bookkeeping (Global Carbon Budget, Friedlingstein et al., 2019). The long-term record (1960–2018) provides a constraint on the global simulated C cycle.
165 All the models are on the correct order of magnitude for NEP and capture the upward trend post 1980 (Fig. 2). JULES is the most accurate model by the GCB measure of NEP, having more years within the bookkeeping constraints than the other models.

The non-N model structure strongly influences NEP; CLM5 and CLM4.5 are the two lowest representations of NEP and follow a similar trajectory (Fig. 2). The CLM models share many model components and this common functioning appears
170 to dominate the signal for NEP. This contrast with GPP, where despite the similarities between CLM4.5 and CLM5 they are not as close in global total as in NEP and have significant differences in spatial pattern (Figs. 1 and 3). This is because while the GPP is heavily influenced by the N cycles in these models, the respiration terms are similarly affected by N and thus result in similar patterns of NEP.

Across the ensemble there is a slight correlation between the global GPP total and NEP. LPJ-GUESS is the highest GPP and
175 highest NEP in the majority of years in the period 1970–2010. Similarly, although CLM5 has the lowest NEP in the same period, CLM4.5 has only slightly more NEP. JSBACH is the second highest global total amongst the models for NEP and GPP. Compared to GPP, including the respiration in this global metric increases the spread of models, reflecting increased uncertainties with increased processes considered.

3.1.1 Global C and N budget

180 Looking at a range of pools and fluxes emphasises the similarities between the models (see Fig. 3). We use the closest comparable observation-based data to look at the flow of model C and N. The C input of GPP is generally better represented by the models than this flow chart would indicate. In the interests of consistency, we've used 1996–2005 as the baseline for GPP, but when the directly comparable period is used (as in Fig. 1) all the models are well within the uncertainty boundaries.
[Fig 3. Flux/Pool flow chart]

185 The N inputs of deposition and BNF show that most of the uncertainty for N input comes from BNF (Fig. 3). Deposition is a prescribed input with very little variation. BNF on the other hand has a wider observed range, and one model is still outside of it. The three models with the highest BNF (JSBACH, CLM5, and JULES) use NPP based function to calculate BNF. JULES and JSBACH are based on Cleveland (1999)'s empirical large-scale correlation with net primary productivity (NPP). LPJ-GUESS, the lowest BNF model, also uses an empirical correlation from Cleveland (1999), based on evapotranspiration
190 rather than NPP. Thus, even BNF functions from the same source can have very different results (Wieder et al., 2015a), due to the large range of BNF functions and differences in how they are implemented. BNF dominates N input variability both because of lack of process understanding to constrain model structures and the continued large uncertainty in available observations.



The respiration terms are consistent across all the models, with two errors cancelling each other out. Autotrophic respiration is overestimated in all the models, by up to ~50% of the observed value (Luysaert et al., 2014; Piao et al., 2010). Heterotrophic respiration is underestimated in all the models, by as much as ~20% compared to the observed values from Bond-Lamberty and Thomson, (2010). The observed value (Bond-Lamberty and Thomson, 2010) is, however, reduced by 33% to account for root respiration, in line with Bowden et al., (1993). Overall, the underestimation of heterotrophic respiration fully compensates for the overestimate of autotrophic respiration. Looking at total observed respiration (102 – 200 128 PgC yr⁻¹) all the models are within that range.

N losses via gaseous loss to the atmosphere and leaching to groundwater / rivers are not well constrained globally (Galloway et al., 2004). However, the models have a limited range of N loss values. Looking at inputs and losses excluding anthropogenic N addition (BNF + N Deposition – N Loss), all the models have a surplus of N and could be said to be ‘open’ systems with regard to N balance.

The stocks of C and N are less well constrained and have a larger inter-model range than the fluxes. The Vegetation C is generally high and the Soil+Litter C is generally low, compared to observational estimates from Carvalhais et al., (2014). Despite the large range, three of five models are under observation range (white arrows, Fig. 3). The C and N in the vegetation are not strongly correlated, with the model with the highest VegC having a middle of the model range VegN (JULES). Comparing the C:N of Soil+Litter global total weight the ratios are similar across models, around 11-13:1 C:N and 210 JSBACH 18:1. The higher ratio for JSBACH is due to the 10:1 ratio for slowly decomposing soil carbon (humus) and larger ratio for litter. Overall, the flux values are both better known and represented, while the pools are more variable and have fewer global comparators.

3.1 Modelled Responses to +N and +CO₂ Experiments

The +N and +CO₂ perturbation experiments (described in the methods) are designed to mimic field experiments undertaken to understand the effects of elevated CO₂ or N. These simulations reveal the overall pattern of response of the model to these forcings. Ideally the models would capture the global and regional signals, as indicated by the observed data. However, comparisons between models alone can also provide useful insight into the models’ behaviour.

All the models except CLM4.5 (which has a low response) capture the global mean response of NPP to +CO₂ within the range of observations (Fig. 4). CLM4.5 has proportionally high response in arid areas of North Africa and central Asia, but 220 the absolute values of NPP in these regions are low.

Regional patterns in response vary considerably for key biomes. +CO₂ response ranges between none (JULES) and high (CLM5) for high latitude tundra areas which have little vegetation carbon in the present day but are critical in future climate change scenarios. Model responses of NPP to +CO₂ in greater Amazonia also don’t reach a consensus. Comparing the response in the Amazonia region with that of coastal regions of northern South America, the JSBACH response is lower, 225 CLM5 and LPJ-GUESS higher, and JULES and CLM4.5 are approximately the same. The NPP response of Amazonia to



+CO₂ ranges from ~10% for CLM4.5 to ~30% for CLM5 and LPJ-GUESS. Therefore, although the models reach a majority consensus on +CO₂ NPP effects overall, the important regional details are still contradictory.

The response to +N in the models shows a wider spread than for +CO₂ or the control scenario, with 3/5 models outside of the observed limits for NPP response (Fig. 5). JSBACH and JULES have global NPP responses to +N of 2.3% and 2.6% respectively. For JSBACH, this is explained by the concept of CO₂-induced nitrogen limitation (Goll et al., 2017) which assumes an absence of N limitation in pre-industrial state due to long-term plant adaptation to environment during the Holocene. CLM4.5 has the highest response, on account of its very high initial N limitation, at 25%. However, even within models with similar levels of +N response, there are regional differences in distribution.

The most prevalent spatial trend is regions either having sensitivity to +N or +CO₂, but not both (see Fig. 4 and 5). This is most pronounced in JULES, where high latitude regions have a response to +N but no response to +CO₂. However, to a lesser extent this is also seen in CLM4.5, CLM5, and LPJ-GUESS. Wieder et al., (2019) also found that there was a trade-off between +N impact and +CO₂ impact in CLM4, CLM4.5 and CLM5. There is spatial pattern and global total similarity between CLM4.5 and CLM5 in their NPP response to +N, in contrast to their differing responses to +CO₂. Only JSBACH doesn't appear to have a dichotomy between +N and +CO₂ response.

Although the models generally have lower than observed global NPP response to +N, regionally there are areas of over and underestimation. Tundra biome response is high in CLM5 and JULES, and present in LPJ-GUESS and CLM4.5 (Fig. 5). This is an overestimation of the observed 35% N fertilisation response (LeBauer and Treseder, 2008). Conversely, the +N response of temperate grassland (53%) (LeBauer and Treseder, 2008) is underestimated by all the models, with JULES and JSBACH showing less than 20% response in most temperate areas. There is a high response to +N in Africa & Australia in CLM4.5, CLM5, and LPJ-GUESS, despite aridity likely limiting increase in NPP in absolute, if not relative, terms. One area of agreement between the models is the lack of +N response in the tropics, especially over the Amazonian region. This is also consistent with observations which show just a 5% non-significant +N response in the tropics (Schulte-Uebbing and Vries, 2018). With the exception of the tropics, the models are underestimating the global +N response and showing the response in biomes inconsistent with the observations.

The models' responses in different parts of the N budget affect their overall N sensitivity (Fig. 6). N inputs of BNF and N deposition and loss (we only consider the sum of leaching and gaseous loss to be consistent between models) are very similar between all the models in the Control simulation. This leads to small differences in the N balance between the models. The N balance appears to be weakly anti-correlated with total GPP (see Fig. 1f and Fig. 6a). However, the uptake of N varies a lot more between models, reflecting differing levels of N mineralisation, model structure, and assumed N requirements.

The largest responses to +N and +CO₂ of input and loss do not necessarily correlate with either N uptake or changes to productivity. The weak response of NPP to +CO₂ in CLM4.5 would suggest only small changes in uptake compared to the other models (Fig. 4). However, the +CO₂ induced changes in BNF, loss, N balance and uptake CLM4.5 are approximately middle of the model range (Fig. 6). CLM5 has a large increase in N balance from BNF and decreased loss (positive change in gaseous loss and leaching in Fig. 6b) but decreased uptake. This is due to a model feature that CLM considers BNF as N



260 delivery to the plant by nodules, and thus doesn't count it as uptake from the soil. CO₂ fertilisation increases BNF in CLM5 due to the cost based portioning of C expenditure on N uptake that reduces the active uptake of mineralised N and increases BNF when soil N stocks are low (on account of increased growth from +CO₂) (Fisher et al., 2010, 2018).

The uptake changes in JULES and JSBACH reflect their sensitivity to +N and +CO₂. These models have the highest uptake changes for +CO₂ and the smallest uptake changes for +N (Fig. 6). For JULES we can see that this is driven by changes in
265 loss, particularly for +N, which leads to a much smaller increase in N balance in JULES than the other models. In common with all the models, in JULES the N loss term is a fixed fraction of the mineralisation flux and the soil N pool size. In contrast, JSBACH has less than half the increase in loss of JULES in the +N simulation (Fig. 6c) and almost no change in NUE (Fig. 7d). This suggests that in both JULES and JSBACH there is effectively very little unmet N demand in the Control scenario and whereas JULES loses the extra N, JSBACH retains it in the soil.

270 Two of the most important factors for plants' use of N are the availability and demand for N use. The variability of these processes is determined primarily by the BNF and NUE respectively, which are both known to be affected by increased CO₂ and N. Neither BNF nor NUE are well constrained by observations and thus show heterogeneity of response between models. The models come to quite similar global results (e.g. for GPP (Fig. 1) or NPP +CO₂ response (Fig. 4)) through very different NUE and BNF behaviours (Fig. 7).

275 The BNF responses to +CO₂ of the models differ from the average response recorded in a global meta-analysis of CO₂ manipulation (Liang et al., 2016) (Fig. 7a). The observation here is an upscaling of studies rather than a representative global observation and therefore the comparison needs to be interpreted accordingly. Only JULES' responses in all regions except boreal and CLM5's boreal response are within the range of the meta-analysis. CLM5 is a clear outlier, with a large increase in BNF as it takes a C cost approach to estimated BNF which is different to the other models (Table 1). BNF can be acquired
280 for a relatively fixed amount of C (Houlton et al., 2008), when C availability increases under +CO₂ the BNF, in this case more than field data would suggest. Fisher et al., (2018) conduct a parameter sensitivity analysis of both +CO₂ and +N fertilization and illustrate that both responses are sensitive to the maximum fraction of carbon which is available for fixation (a proxy for the fraction of N fixing plants) and thus this response might be due to this.

The models' BNF response to +N shows one of two responses: a small increase in JULES, CLM4.5, and JSBACH; or a large
285 decrease in CLM5 and LPJ-GUESS (Fig. 7). The latter models capture the correct BNF sign of response to +N of a decrease, though the amplitude is too high. The former models estimate BNF as a function of NPP which results in increased BNF whatever the source of the additional NPP is. This gives a counter-intuitive BNF response of more BNF being produced, even though there is already sufficient N. Overall, there is little evidence for any of the BNF algorithms performing well.

The NUE responses allow comparison between models, though comparisons with observations are limited by lack of field
290 studies. The NUE responses of the models are similar to that of BNF, with CLM5 having the largest response to +CO₂ and CLM4.5 the smallest (Fig. 7). All models have an increase in NUE with +CO₂, which is in line with current theory (Walker et al., 2015). CLM4.5 has low NUE response to +CO₂ due to fixed C:N ratios, which allow little change in NUE. The other



models allow either more allocation to wood or flexible C:N that results in the larger increases of NUE. CLM5 has large changes in NUE because BNF is not considered as uptake.

295 There is regional variation in NUE response to +N between biomes in some models. CLM5 and LPJ-GUESS are distinct in their response to +N compared to the other models, but do not share the same geographical spread of response. JSBACH, LPJ-GUESS, and CLM4.5 all have globally consistent responses. JULES and CLM5 have more spatial variation, with different responses between boreal and tropical regions. All the models except JULES reduce NUE in response to +N. Though no empirical measurements are currently available for NUE response to +N, it seems more likely that NUE would

300 increase when N was scarce and vice versa. The large variations in signal and sign of BNF and NUE response between models suggests there is still progress to be made.

We can gain further insights by considering the relationship between the response to +CO₂ and +N (Fig. 8). The ideal for the models is to be in the area where the observations for +N and +CO₂ intersect. Two of the models achieve this partially, JSBACH and CLM5, by having tightly clustered vegetation C (VegC) response to +N and NPP response to +CO₂. One

305 model, CLM4.5 has all three biomes outside of both the +N and +CO₂ observational ranges.

[Figure 8 +N vs +CO₂]

It might be anticipated there would be a relationship between the two responses, as an ecosystem (model) that is less N limited would be expected to respond more strongly to increased atmospheric CO₂. However, the models show little relationship between the +N response and +CO₂ response (Fig. 8). At a regional level the models either vary in +N response

310 but not +CO₂ (LPJ-GUESS and CLM4.5) or vary little in either (JULES, JSBACH and CLM5).

According to observations we would expect models to have biome differences in +N response, but none of the models correctly capture this (Fig. 8). All the models except LPJ-GUESS and CLM4.5 have tropical +N response in the correct range (Fig. 8). LPJ-GUESS is the only model to have the boreal +N response in the correct range. The observations from N addition experiments (Schulte-Uebbing and Vries, 2018) show lower tropical +N response than boreal or temperate, but none

315 of the models have the biome responses in the correct order. It is the boreal response that seems to be the main issue, as most of the models show increased +N response compared to the tropics for temperate regions, but dampened response for boreal regions. Therefore, although the global values of response are acceptable, the relative spatial patterns show limitations in the reliability of all the models.

4 Discussion

320 This second generation of N models in CMIP do well at reproducing key global metrics, such as GPP and NEP and generally show magnitudes of responses to increased atmospheric CO₂ commensurate with those recorded in field studies. The response to N addition is more varied. Though there is considerable variation in the values for many fluxes and pools, the models tend to represent net fluxes well where they are constrained by observations. In the case of respiration, overestimates of autotrophic and underestimates of heterotrophic respiration combine to give good overall agreement. The fluxes are



325 generally better represented by the models than the pools, possibly due to the tighter observational constraints on fluxes. However, the N processes have considerable heterogeneity and there are regional differences in the robustness of response. Two models of the five (JULES and JSBACH) have virtually no productivity response to increased N availability, suggesting they don't have any significant N limitation (Fig. 5). There are four substantial similarities between these two models (Table 1): the use of NPP to determine BNF; GPP is not directly affected by N; the use of dynamic (as oppose to
330 prescribed) vegetation; and the assumption of no pre-industrial N limitation. Since we lack observations of N limitation for the pre-industrial period, the assumption that increases in atmospheric CO₂ are the cause of N limitation in the present day is difficult to disprove. However, this assumption drives other model decisions (such as N limitation not being incorporated into the GPP equation, see Table 1), which appear to lead to models being under-sensitive to N compared to observations.

We have focused on three general parts of N models that affect the N uptake and eventual productivity: N inputs via BNF;
335 NUE; and the N losses. We find that all three show considerable heterogeneity of response between models. Previous studies suggest that stoichiometric controls and the processing of soil organic matter are important for a realistic +CO₂ response (Zaehle et al., 2014a). These are essentially contributory factors to NUE, where we find large variation between models. The lack of well constrained observations for global and biome-level NUE and N loss responses make these areas that need more work. N loss is particularly challenging, as there are multiple paths (leaching, flooding, gaseous loss, fire, land use change,
340 etc.) and forms (N₂O, N₂, etc.) of loss and each model represents these in different ways. More observational studies and syntheses of existing observations are needed to quantify the nitrogen cycle in different biomes. In particular, better constraints are needed for the N cycle response to perturbations.

The models mostly represent high latitude northern hemisphere regions less well than other parts of the world, in part because of the unique challenges these areas set for models. We see in Fig. 8 that the N response of the boreal biome is
345 underestimated, and in Fig. 5 the conflicting predictions of N response in the very high latitudes. High latitude tundra is a critical but difficult to model biome because of the potential for release of methane (Nauta et al., 2015), permafrost C and N release (Anisimov, 2007; Burke et al., 2012; O'Connor et al., 2010), and albedo changes with vegetation expansion (Myers-Smith et al., 2011) and the difficulty in representing large amounts of C stored in soil. This partly accounts for why tundra NPP response to +N is overestimated in all the models, because the processes in this biome are complex, but differing
350 vegetation representation may also contribute. If +CO₂ does increase NPP in tundra areas, the substantial biogeophysical albedo changes may be larger than the carbon changes (Betts, 2000; Cohen et al., 2013). Tundra is a low productivity area and though the absolute change from +N or +CO₂ is small, as a proportion it is large and could have wide ranging effects. A fully integrated model that accounts correctly for all of these is not yet possible, but is necessary to reduce uncertainties.

The northern part of South America of the greater Amazon basin is a critical area of interest for LSMs under climate change.
355 The NPP in this area increases in some of the models for +CO₂, but all the models find a small or no change in NPP with +N. The +N response is small because the favourable conditions already give a high leaf area index (LAI) in this part of the tropics, and there is little margin for increased NPP (Fisher et al., 2018). For +CO₂ there is the potential for increased NPP because the NUE increases, giving productivity increase without an increase in LAI. However, reducing the uncertainty in



360 NPP response to +CO₂ is important, as the moist tropics represent a significant proportion of the world's aboveground biomass and therefore the size of the overall terrestrial sink will be influenced by the CO₂ uptake in this biome.

Part of the uncertainty in the models comes from the reanalysis climate dataset used to drive the models. CRU-NCEP was chosen for the good spatial and temporal coverage, but some biases exist in the data compared to climatologies such as WATCH (Weedon et al., 2011). Offline simulations driven by low forcing frequency (six-hourly) CRU-NCEP data significantly overestimate evapotranspiration in regions with convective rainfall types and thereby could affect stomatal conductance and photosynthesis (Fan et al., 2019). This does not affect all the models equally, as some are more sensitive to the driving climatology. JSBACH's performance is particularly affected by CRU-NCEP, and JULES and LPJ-GUESS may also be strongly affected due to its dynamic vegetation. Lawrence et al. (2019) show that CLM5 corresponds best to benchmarks with GSWP3 forcing dataset (Hurk et al., 2016). Responses may partially be shaped by other limiting factors such as water availability, which will be handled differently between models limiting the insight on the exact processes that control model responses to change. The climatology should have a small effect on the model response but may skew the global values the models with dynamic vegetation since the biomes may be incorrectly represented globally.

As well as uncertainty in the models, the observational data also has uncertainties. Global benchmarks are approximate measures, as multi-faceted process mechanics are integrated over large domains and generalized, e.g., over climate zones that are inherently variable. Of the limited global or regional observations available, many use interpolation or proxies such as satellite data to upscale relatively small amounts of direct observational data. In particular, the perturbed responses have uncertainties beyond the spread of the observed responses because of the small observation basis and potential biases in the geographical sampling. The +N global response cited is based on 126 values from LeBauer and Treseder, (2008) but may over-estimate the global response by including high responses from young tropical soils. The NPP response to +CO₂ response is based on just 23 experiments, of which only few have been conducted at field scale (Baig et al., 2015). Similarly, the accuracy of global GPP data from satellite data is based on modelling assumptions that convert observations to GPP values (Koirala et al. forthcoming). Hence statements about the marginal issues of model accuracy are unlikely to be robust as further observational constraints may alter the perspective.

5 Conclusions

This is the first systematic comparison of the responses to N and CO₂ in LSMs with terrestrial N cycles used within the CMIP6 endeavour. CMIP6 models with interactive N cycling show a reduction in carbon feedback uncertainty comparing to a carbon-only models (Arora et al., 2019). Our analysis elucidates some of the strengths and weaknesses of LSMs that include an N cycle. The five models considered here have good overall agreement with global and tropical observations but are less robust in high latitude regions.

The models are not equally sensitive to either +CO₂ or +N, with responses varying by up to an order of magnitude. CLM4.5 has very low NPP response to +CO₂, and JULES and JSBACH has a low NPP response to +N. Though CLM5 performs



well by many metrics, it has large BNF and NUE responses to CO₂. Similarly, LPJ-GUESS captures NPP responses to +CO₂ and +N well at the global level but overestimates the VegC response to +N in non-forested tropical and temperate biomes. The wide range of empirical or semi-mechanistic representations for key processes such as BNF, NUE, and N loss, show how important further process understanding is for many parts of the N cycle. These parts of the models are influential, but because N cycle components are a recent addition to LSMs, fewer data are available than for carbon cycle components. Despite a larger range of observational datasets, the carbon cycle pools are not well constrained and have large differences between models, especially for the soil carbon pools. Consequently, better observational constraints are required to understand whether models are working appropriately, even where the process understanding is improved.

Acknowledgements

Data used to generate the figures, plots, and tables in this paper will be archived on the University of Exeter repository upon publication in line with the appropriate guidelines.

Authors acknowledge funding from the European Union's Horizon 2020 research and innovation programme under grant agreement No. 641816 Coordinated Research in Earth Systems and Climate: Experiments kNowledge, Dissemination and Outreach (CRESCENDO).

SZ acknowledges support by the European Union's Horizon 2020 research and innovation programme under grant agreement No. 647204 (QUINCY).

PF acknowledges funding from the European Union's Horizon 2020 research and innovation programme under grant agreement No. 821003 (4C project).

RF was supported by the National Center for Atmospheric Research, which is a major facility sponsored by the NSF under Cooperative Agreement 1852977.

BS acknowledges this study is a contribution to the Strategic Research Area MERGE.

References

Anav, A., Friedlingstein, P., Kidston, M., Bopp, L., Ciais, P., Cox, P., Jones, C., Jung, M., Myneni, R. and Zhu, Z.: Evaluating the Land and Ocean Components of the Global Carbon Cycle in the CMIP5 Earth System Models, *J. Climate*, 26(18), 6801–6843, doi:10.1175/JCLI-D-12-00417.1, 2013.

Anisimov, O. A.: Potential feedback of thawing permafrost to the global climate system through methane emission, *Environ. Res. Lett.*, 2(4), 045016, doi:10.1088/1748-9326/2/4/045016, 2007.

Arora, V. K., Boer, G. J., Friedlingstein, P., Eby, M., Jones, C. D., Christian, J. R., Bonan, G., Bopp, L., Brovkin, V., Cadule, P., Hajima, T., Ilyina, T., Lindsay, K., Tjiputra, J. F. and Wu, T.: Carbon–Concentration and Carbon–Climate Feedbacks in CMIP5 Earth System Models, *J. Climate*, 26(15), 5289–5314, doi:10.1175/JCLI-D-12-00494.1, 2013.



- Arora, V. K., Katavouta, A., Williams, R. G., Jones, C. D., Brovkin, V., Friedlingstein, P., Schwinger, J., Bopp, L., Boucher, O., Cadule, P., Chamberlain, M. A., Christian, J. R., Delire, C., Fisher, R. A., Hajima, T., Ilyina, T., Joetzjer, E., Kawamiya, M., Koven, C., Krasting, J., Law, R. M., Lawrence, D. M., Lenton, A., Lindsay, K., Pongratz, J., Raddatz, T., Séférian, R., Tachiiri, K., Tjiputra, J. F., Wiltshire, A., Wu, T. and Ziehn, T.: Carbon-concentration and carbon-climate feedbacks in
425 CMIP6 models, and their comparison to CMIP5 models, *Biogeosciences Discussions*, 1–124, doi:<https://doi.org/10.5194/bg-2019-473>, 2019.
- Baig, S., Medlyn, B. E., Mercado, L. M. and Zaehle, S.: Does the growth response of woody plants to elevated CO₂ increase with temperature? A model-oriented meta-analysis, *Global Change Biology*, 21(12), 4303–4319, doi:10.1111/gcb.12962, 2015.
- 430 Best, M. J., Pryor, M., Clark, D. B., Rooney, G. G., Essery, R. L. H., Ménard, C. B., Edwards, J. M., Hendry, M. A., Porson, A. and Gedney, N.: The Joint UK Land Environment Simulator (JULES), model description–Part 1: energy and water fluxes, *Geoscientific Model Development*, 4(3), 677–699, 2011.
- Betts, R. A.: Offset of the potential carbon sink from boreal forestation by decreases in surface albedo, *Nature*, 408(6809), 187–190, doi:10.1038/35041545, 2000.
- 435 Bonan, G. B., Oleson, K. W., Fisher, R. A., Lasslop, G. and Reichstein, M.: Reconciling leaf physiological traits and canopy flux data: Use of the TRY and FLUXNET databases in the Community Land Model version 4, *Journal of Geophysical Research: Biogeosciences*, 117(G2), doi:10.1029/2011JG001913, 2012.
- Bond-Lamberty, B. and Thomson, A.: A global database of soil respiration data, *Biogeosciences*, 7(6), 1915–1926, doi:<https://doi.org/10.5194/bg-7-1915-2010>, 2010.
- 440 Bowden, R. D., Nadelhoffer, K. J., Boone, R. D., Melillo, J. M. and Garrison, J. B.: Contributions of aboveground litter, belowground litter, and root respiration to total soil respiration in a temperate mixed hardwood forest, *Can. J. For. Res.*, 23(7), 1402–1407, doi:10.1139/x93-177, 1993.
- Burke, E. J., Hartley, I. P. and Jones, C. D.: Uncertainties in the global temperature change caused by carbon release from permafrost thawing, *The Cryosphere*, 6(5), 1063–1076, doi:10.5194/tc-6-1063-2012, 2012.
- 445 Carvalhais, N., Forkel, M., Khomik, M., Bellarby, J., Jung, M., Migliavacca, M., Mu, M., Saatchi, S., Santoro, M., Thurner, M., Weber, U., Ahrens, B., Beer, C., Cescatti, A., Randerson, J. T. and Reichstein, M.: Global covariation of carbon turnover times with climate in terrestrial ecosystems, *Nature*, 514(7521), 213–217, doi:10.1038/nature13731, 2014.
- Cherchi, A., Fogli, P. G., Lovato, T., Peano, D., Iovino, D., Gualdi, S., Masina, S., Scoccimarro, E., Materia, S., Bellucci, A. and Navarra, A.: Global Mean Climate and Main Patterns of Variability in the CMCC-CM2 Coupled Model, *Journal of*
450 *Advances in Modeling Earth Systems*, 11(1), 185–209, doi:10.1029/2018MS001369, 2019.
- Clark, D. B., Mercado, L. M., Sitch, S., Jones, C. D., Gedney, N., Best, M. J., Pryor, M., Rooney, G. G., Essery, R. L. H., Blyth, E., Boucher, O., Harding, R. J., Huntingford, C. and Cox, P. M.: The Joint UK Land Environment Simulator (JULES), model description – Part 2: Carbon fluxes and vegetation dynamics, *Geoscientific Model Development*, 4(3), 701–722, doi:10.5194/gmd-4-701-2011, 2011.



- 455 Cohen, J., Pulliainen, J., Ménard, C. B., Johansen, B., Oksanen, L., Luojus, K. and Ikonen, J.: Effect of reindeer grazing on snowmelt, albedo and energy balance based on satellite data analyses, *Remote Sensing of Environment*, 135, 107–117, doi:10.1016/j.rse.2013.03.029, 2013.
- Eyring, V., Bony, S., Meehl, G. A., Senior, C. A., Stevens, B., Stouffer, R. J. and Taylor, K. E.: Overview of the Coupled Model Intercomparison Project Phase 6 (CMIP6) experimental design and organization, *Geoscientific Model Development*, 9(5), 1937–1958, doi:<https://doi.org/10.5194/gmd-9-1937-2016>, 2016.
- 460 Fan, Y., Meijide, A., Lawrence, D. M., Rouspard, O., Carlson, K. M., Chen, H.-Y., Röhl, A., Niu, F. and Knohl, A.: Reconciling Canopy Interception Parameterization and Rainfall Forcing Frequency in the Community Land Model for Simulating Evapotranspiration of Rainforests and Oil Palm Plantations in Indonesia, *Journal of Advances in Modeling Earth Systems*, 11(3), 732–751, doi:10.1029/2018MS001490, 2019.
- 465 Fisher, J. B., Sitch, S., Malhi, Y., Fisher, R. A., Huntingford, C. and Tan, S.-Y.: Carbon cost of plant nitrogen acquisition: A mechanistic, globally applicable model of plant nitrogen uptake, retranslocation, and fixation, *Global Biogeochem. Cycles*, 24(1), GB1014, doi:10.1029/2009GB003621, 2010.
- Fisher, R. A., Wieder, W. R., Sanderson, B. M., Koven, C. D., Oleson, K. W., Xu, C., Fisher, J. B., Shi, M., Walker, A. P. and Lawrence, D. M.: Parametric Controls on Vegetation Responses to Biogeochemical Forcing in the CLM5, *Journal of Advances in Modeling Earth Systems*, 2879–2895, doi:10.1029/2019MS001609@10.1002/(ISSN)1942-2466.CESM2, 2018.
- 470 Friedlingstein, P., Cox, P., Betts, R., Bopp, L., Von Bloh, W., Brovkin, V., Cadule, P., Doney, S., Eby, M. and Fung, I.: Climate-carbon cycle feedback analysis: Results from the C4MIP model intercomparison, *Journal of Climate*, 19(14), 3337–3353, 2006.
- Friedlingstein, P., Jones, M. W., O’Sullivan, M., Andrew, R. M., Hauck, J., Peters, G. P., Peters, W., Pongratz, J., Sitch, S., Quéré, C. L., Bakker, D. C. E., Canadell, J. G., Ciais, P., Jackson, R. B., Anthoni, P., Barbero, L., Bastos, A., Bastrikov, V., 475 Becker, M., Bopp, L., Buitenhuis, E., Chandra, N., Chevallier, F., Chini, L. P., Currie, K. I., Feely, R. A., Gehlen, M., Gilfillan, D., Gkritzalis, T., Goll, D. S., Gruber, N., Gutekunst, S., Harris, I., Haverd, V., Houghton, R. A., Hurtt, G., Ilyina, T., Jain, A. K., Joetzjer, E., Kaplan, J. O., Kato, E., Klein Goldewijk, K., Korsbakken, J. I., Landschützer, P., Lauvset, S. K., Lefèvre, N., Lenton, A., Lienert, S., Lombardozzi, D., Marland, G., McGuire, P. C., Melton, J. R., Metzl, N., Munro, D. R., 480 Nabel, J. E. M. S., Nakaoka, S.-I., Neill, C., Omar, A. M., Ono, T., Peregon, A., Pierrot, D., Poulter, B., Rehder, G., Resplandy, L., Robertson, E., Rödenbeck, C., Séférian, R., Schwinger, J., Smith, N., Tans, P. P., Tian, H., Tilbrook, B., Tubiello, F. N., Werf, G. R. van der, Wiltshire, A. J. and Zaehle, S.: Global Carbon Budget 2019, *Earth System Science Data*, 11(4), 1783–1838, doi:<https://doi.org/10.5194/essd-11-1783-2019>, 2019.
- Galloway, J. N., Dentener, F. J., Capone, D. G., Boyer, E. W., Howarth, R. W., Seitzinger, S. P., Asner, G. P., Cleveland, C. 485 C., Green, P. A., Holland, E. A., Karl, D. M., Michaels, A. F., Porter, J. H., Townsend, A. R. and Vöosmarty, C. J.: Nitrogen Cycles: Past, Present, and Future, *Biogeochemistry*, 70(2), 153–226, doi:10.1007/s10533-004-0370-0, 2004.



- Goll, D. S., Winkler, A. J., Raddatz, T., Dong, N., Prentice, I. C., Ciais, P. and Brovkin, V.: Carbon–nitrogen interactions in idealized simulations with JSBACH (version 3.10), *Geoscientific Model Development*, 10(5), 2009–2030, doi:<https://doi.org/10.5194/gmd-10-2009-2017>, 2017.
- 490 Hazeleger, W., Wang, X., Severijns, C., Ștefănescu, S., Bintanja, R., Sterl, A., Wyser, K., Semmler, T., Yang, S., van den Hurk, B., van Noije, T., van der Linden, E. and van der Wiel, K.: EC-Earth V2.2: description and validation of a new seamless earth system prediction model, *Clim Dyn*, 39(11), 2611–2629, doi:10.1007/s00382-011-1228-5, 2012.
- Houlton, B. Z., Wang, Y.-P., Vitousek, P. M. and Field, C. B.: A unifying framework for dinitrogen fixation in the terrestrial biosphere, *Nature*, 454(7202), 327–330, doi:10.1038/nature07028, 2008.
- 495 Hurk, B. van den, Kim, H., Krinner, G., Seneviratne, S. I., Derksen, C., Oki, T., Douville, H., Colin, J., Ducharne, A., Cheruy, F., Viovy, N., Puma, M. J., Wada, Y., Li, W., Jia, B., Alessandri, A., Lawrence, D. M., Weedon, G. P., Ellis, R., Hagemann, S., Mao, J., Flanner, M. G., Zampieri, M., Materia, S., Law, R. M. and Sheffield, J.: LS3MIP (v1.0) contribution to CMIP6: the Land Surface, Snow and Soil moisture Model Intercomparison Project – aims, setup and expected outcome, *Geoscientific Model Development*, 9(8), 2809–2832, doi:<https://doi.org/10.5194/gmd-9-2809-2016>, 2016.
- 500 Hurtt, G., Chini, L., Frohking, S., Betts, R., Feddema, J., Fischer, G., Fisk, J., Hibbard, K., Houghton, R., Janetos, A., Jones, C., Kindermann, G., Kinoshita, T., Klein Goldewijk, K., Riahi, K., Shevliakova, E., Smith, S., Stehfest, E., Thomson, A., Thornton, P., van Vuuren, D. and Wang, Y.: Harmonization of land-use scenarios for the period 1500–2100: 600 years of global gridded annual land-use transitions, wood harvest, and resulting secondary lands, *Climatic Change*, 109(1), 117–161, doi:10.1007/s10584-011-0153-2, 2011.
- 505 Jones, C., Robertson, E., Arora, V., Friedlingstein, P., Shevliakova, E., Bopp, L., Brovkin, V., Hajima, T., Kato, E., Kawamiya, M., Liddicoat, S., Lindsay, K., Reick, C. H., Roelandt, C., Segschneider, J. and Tjiputra, J.: Twenty-First-Century Compatible CO₂ Emissions and Airborne Fraction Simulated by CMIP5 Earth System Models under Four Representative Concentration Pathways, *J. Climate*, 26(13), 4398–4413, doi:10.1175/JCLI-D-12-00554.1, 2013.
- Jung, M., Reichstein, M., Margolis, H. A., Cescatti, A., Richardson, A. D., Arain, M. A., Arneeth, A., Bernhofer, C., Bonal, D., Chen, J., Gianelle, D., Gobron, N., Kiely, G., Kutsch, W., Lasslop, G., Law, B. E., Lindroth, A., Merbold, L., Montagnani, L., Moors, E. J., Papale, D., Sottocornola, M., Vaccari, F. and Williams, C.: Global patterns of land-atmosphere fluxes of carbon dioxide, latent heat, and sensible heat derived from eddy covariance, satellite, and meteorological observations, *Journal of Geophysical Research: Biogeosciences*, 116(G3), doi:10.1029/2010JG001566, 2011.
- Kennedy, D., Swenson, S., Oleson, K. W., Lawrence, D. M., Fisher, R., Costa, A. C. L. da and Gentine, P.: Implementing Plant Hydraulics in the Community Land Model, Version 5, *Journal of Advances in Modeling Earth Systems*, 11(2), 485–513, doi:10.1029/2018MS001500, 2019.
- 515 Koven, C. D., Riley, W. J., Subin, Z. M., Tang, J. Y., Torn, M. S., Collins, W. D., Bonan, G. B., Lawrence, D. M. and Swenson, S. C.: The effect of vertically resolved soil biogeochemistry and alternate soil C and N models on C dynamics of CLM4, *Biogeosciences*, 10(11), 7109–7131, doi:<https://doi.org/10.5194/bg-10-7109-2013>, 2013.



- 520 Lamarque, J.-F., Shindell, D. T., Josse, B., Young, P. J., Cionni, I., Eyring, V., Bergmann, D., Cameron-Smith, P., Collins, W. J., Doherty, R., Dalsoren, S., Faluvegi, G., Folberth, G., Ghan, S. J., Horowitz, L. W., Lee, Y. H., MacKenzie, I. A., Nagashima, T., Naik, V., Plummer, D., Righi, M., Rumbold, S. T., Schulz, M., Skeie, R. B., Stevenson, D. S., Strode, S., Sudo, K., Szopa, S., Voulgarakis, A. and Zeng, G.: The Atmospheric Chemistry and Climate Model Intercomparison Project (ACCMIP): overview and description of models, simulations and climate diagnostics, *Geoscientific Model Development*, 6(1), 179–206, doi:<https://doi.org/10.5194/gmd-6-179-2013>, 2013.
- 525 Lawrence, D. M., Fisher, R. A., Koven, C. D., Oleson, K. W., Swenson, S. C., Bonan, G., Collier, N., Ghimire, B., Kampenhout, L. van, Kennedy, D., Kluzek, E., Lawrence, P. J., Li, F., Li, H., Lombardozzi, D., Riley, W. J., Sacks, W. J., Shi, M., Vertenstein, M., Wieder, W. R., Xu, C., Ali, A. A., Badger, A. M., Bisht, G., Broeke, M. van den, Brunke, M. A., Burns, S. P., Buzan, J., Clark, M., Craig, A., Dahlin, K., Drewniak, B., Fisher, J. B., Flanner, M., Fox, A. M., Gentine, P., Hoffman, F., Keppel-Aleks, G., Knox, R., Kumar, S., Lenaerts, J., Leung, L. R., Lipscomb, W. H., Lu, Y., Pandey, A., Pelletier, J. D., Perket, J., Randerson, J. T., Ricciuto, D. M., Sanderson, B. M., Slater, A., Subin, Z. M., Tang, J., Thomas, R. Q., Martin, M. V. and Zeng, X.: The Community Land Model Version 5: Description of New Features, Benchmarking, and Impact of Forcing Uncertainty, *Journal of Advances in Modeling Earth Systems*, n/a(n/a), doi:10.1029/2018MS001583, 2020.
- 530 Le Quéré, C. L., Andrew, R. M., Friedlingstein, P., Sitch, S., Hauck, J., Pongratz, J., Pickers, P. A., Korsbakken, J. I., Peters, G. P., Canadell, J. G., Arneeth, A., Arora, V. K., Barbero, L., Bastos, A., Bopp, L., Chevallier, F., Chini, L. P., Ciais, P., Doney, S. C., Gkritzalis, T., Goll, D. S., Harris, I., Haverd, V., Hoffman, F. M., Hoppema, M., Houghton, R. A., Hurtt, G., Ilyina, T., Jain, A. K., Johannessen, T., Jones, C. D., Kato, E., Keeling, R. F., Goldewijk, K. K., Landschützer, P., Lefèvre, N., Lienert, S., Liu, Z., Lombardozzi, D., Metzl, N., Munro, D. R., Nabel, J. E. M. S., Nakaoka, S., Neill, C., Olsen, A., Ono, T., Patra, P., Peregón, A., Peters, W., Peylin, P., Pfeil, B., Pierrot, D., Poulter, B., Rehder, G., Resplandy, L., Robertson, E., Rocher, M., Rödenbeck, C., Schuster, U., Schwinger, J., Séférian, R., Skjelvan, I., Steinhoff, T., Sutton, A., Tans, P. P., Tian, H., Tilbrook, B., Tubiello, F. N., Laan-Luijckx, I. T. van der, Werf, G. R. van der, Viovy, N., Walker, A. P., Wiltshire, A. J., Wright, R., Zaehle, S. and Zheng, B.: Global Carbon Budget 2018, *Earth System Science Data*, 10(4), 2141–2194, doi:<https://doi.org/10.5194/essd-10-2141-2018>, 2018.
- 540 LeBauer, D. S. and Treseder, K. K.: Nitrogen limitation of net primary productivity in terrestrial ecosystems is globally distributed, *Ecology*, 89(2), 371–379, doi:10.1890/06-2057.1, 2008.
- 545 Liang, J., Qi, X., Souza, L. and Luo, Y.: Processes regulating progressive nitrogen limitation under elevated carbon dioxide: a meta-analysis, *Biogeosciences*, 13(9), 2689–2699, doi:<https://doi.org/10.5194/bg-13-2689-2016>, 2016.
- 550 Luysaert, S., Jammert, M., Stoy, P. C., Estel, S., Pongratz, J., Ceschia, E., Churkina, G., Don, A., Erb, K., Ferlicoq, M., Gielen, B., Grünwald, T., Houghton, R. A., Klumpp, K., Knohl, A., Kolb, T., Kuemmerle, T., Laurila, T., Lohila, A., Loustau, D., McGrath, M. J., Meyfroidt, P., Moors, E. J., Naudts, K., Novick, K., Otto, J., Pilegaard, K., Pio, C. A., Rambal, S., Reibmann, C., Ryder, J., Suyker, A. E., Varlagin, A., Wattenbach, M. and Dolman, A. J.: Land management and land-



- cover change have impacts of similar magnitude on surface temperature, *Nature Clim. Change*, 4(5), 389–393, doi:10.1038/nclimate2196, 2014.
- 555 Mauritsen, T., Bader, J., Becker, T., Behrens, J., Bittner, M., Brokopf, R., Brovkin, V., Claussen, M., Crueger, T., Esch, M., Fast, I., Fiedler, S., Fläschner, D., Gayler, V., Giorgetta, M., Goll, D. S., Haak, H., Hagemann, S., Hedemann, C., Hohenegger, C., Ilyina, T., Jahns, T., Jimenéz-de-la-Cuesta, D., Jungclaus, J., Kleinen, T., Kloster, S., Kracher, D., Kinne, S., Kleberg, D., Lasslop, G., Kornbluh, L., Marotzke, J., Matei, D., Meraner, K., Mikolajewicz, U., Modali, K., Möbis, B., Müller, W. A., Nabel, J. E. M. S., Nam, C. C. W., Notz, D., Nyawira, S.-S., Paulsen, H., Peters, K., Pincus, R., Pohlmann, H., Pongratz, J., Popp, M., Raddatz, T. J., Rast, S., Redler, R., Reick, C. H., Rohrschneider, T., Schemann, V., Schmidt, H., Schnur, R., Schulzweida, U., Six, K. D., Stein, L., Stemmler, I., Stevens, B., Storch, J.-S. von, Tian, F., Voigt, A., Vrese, P., Wieners, K.-H., Wilkenskjaeld, S., Winkler, A. and Roeckner, E.: Developments in the MPI-M Earth System Model version 1.2 (MPI-ESM1.2) and Its Response to Increasing CO₂, *Journal of Advances in Modeling Earth Systems*, 11(4), 998–1038, doi:10.1029/2018MS001400, 2019.
- 560 McGroddy, M. E., Daufresne, T. and Hedin, L. O.: Scaling of C:n:p Stoichiometry in Forests Worldwide: Implications of Terrestrial Redfield-Type Ratios, *Ecology*, 85(9), 2390–2401, doi:10.1890/03-0351, 2004.
- Medlyn, B. E., Duursma, R. A., Eamus, D., Ellsworth, D. S., Prentice, I. C., Barton, C. V. M., Crous, K. Y., Angelis, P. D., Freeman, M. and Wingate, L.: Reconciling the optimal and empirical approaches to modelling stomatal conductance, *Global Change Biology*, 17(6), 2134–2144, doi:10.1111/j.1365-2486.2010.02375.x, 2011.
- 570 Meyerholt, J. and Zaehle, S.: The role of stoichiometric flexibility in modelling forest ecosystem responses to nitrogen fertilization, *New Phytologist*, 208(4), 1042–1055, doi:10.1111/nph.13547, 2015.
- Millar, R. J., Fuglestvedt, J. S., Friedlingstein, P., Rogelj, J., Grubb, M. J., Matthews, H. D., Skeie, R. B., Forster, P. M., Frame, D. J. and Allen, M. R.: Emission budgets and pathways consistent with limiting warming to 1.5 °C, *Nature Geoscience*, 10(10), 741–747, doi:10.1038/ngeo3031, 2017.
- 575 Müller, C., Stehfest, E., Minnen, J. G. van, Strengers, B., Bloh, W. von, Beusen, A. H. W., Schaphoff, S., Kram, T. and Lucht, W.: Drivers and patterns of land biosphere carbon balance reversal, *Environ. Res. Lett.*, 11(4), 044002, doi:10.1088/1748-9326/11/4/044002, 2016.
- Myers-Smith, I. H., Forbes, B. C., Wilmking, M., Hallinger, M., Lantz, T., Blok, D., Tape, K. D., Macias-Fauria, M., Sass-Klaassen, U., Lévesque, E., Boudreau, S., Ropars, P., Hermanutz, L., Trant, A., Collier, L. S., Weijers, S., Rozema, J., Rayback, S. A., Schmidt, N. M., Schaepman-Strub, G., Wipf, S., Rixen, C., Ménard, C. B., Venn, S., Goetz, S., Andreu-Hayles, L., Elmendorf, S., Ravolainen, V., Welker, J., Grogan, P., Epstein, H. E. and Hik, D. S.: Shrub expansion in tundra ecosystems: dynamics, impacts and research priorities, *Environ. Res. Lett.*, 6(4), 045509, doi:10.1088/1748-9326/6/4/045509, 2011.
- 580 Nauta, A. L., Heijmans, M. M. P. D., Blok, D., Limpens, J., Elberling, B., Gallagher, A., Li, B., Petrov, R. E., Maximov, T. C., van Huissteden, J. and Berendse, F.: Permafrost collapse after shrub removal shifts tundra ecosystem to a methane source, *Nature Climate Change*, 5(1), 67–70, doi:10.1038/nclimate2446, 2015.



- New, M., Hulme, M. and Jones, P.: Representing Twentieth-Century Space–Time Climate Variability. Part II: Development of 1901–96 Monthly Grids of Terrestrial Surface Climate, *J. Climate*, 13(13), 2217–2238, doi:10.1175/1520-0442(2000)013<2217:RTCSTC>2.0.CO;2, 2000.
- 590 O’Connor, F. M., Boucher, O., Gedney, N., Jones, C. D., Folberth, G. A., Coppel, R., Friedlingstein, P., Collins, W. J., Chappellaz, J., Ridley, J. and Johnson, C. E.: Possible role of wetlands, permafrost, and methane hydrates in the methane cycle under future climate change: A review, *Reviews of Geophysics*, 48(4), doi:10.1029/2010RG000326, 2010.
- Oleson, K. W., Lawrence, D. M., B, G., Flanner, M. G., Kluzek, E., J, P., Levis, S., Swenson, S. C., Thornton, E., Feddema, J., Heald, C. L., Lamarque, J., Niu, G., Qian, T., Running, S., Sakaguchi, K., Yang, L., Zeng, X. and Zeng, X.: Technical
595 Description of version 4.0 of the Community Land Model (CLM)., 2010.
- Olin, S., Lindeskog, M., Pugh, T. a. M., Schurgers, G., Wårlind, D., Mishurov, M., Zaehle, S., Stocker, B. D., Smith, B. and Arneth, A.: Soil carbon management in large-scale Earth system modelling: implications for crop yields and nitrogen leaching, *Earth System Dynamics*, 6(2), 745–768, doi:https://doi.org/10.5194/esd-6-745-2015, 2015.
- Piao, S., Luyssaert, S., Ciais, P., Janssens, I. A., Chen, A., Cao, C., Fang, J., Friedlingstein, P., Luo, Y. and Wang, S.: Forest
600 annual carbon cost: a global-scale analysis of autotrophic respiration, *Ecology*, 91(3), 652–661, doi:10.1890/08-2176.1, 2010.
- Schulte-Uebbing, L. and Vries, W. de: Global-scale impacts of nitrogen deposition on tree carbon sequestration in tropical, temperate, and boreal forests: A meta-analysis, *Global Change Biology*, 24(2), e416–e431, doi:10.1111/gcb.13862, 2018.
- Sellar, A. A., Jones, C. G., Mulcahy, J., Tang, Y., Yool, A., Wiltshire, A., O’Connor, F. M., Stringer, M., Hill, R., Palmieri,
605 J., Woodward, S., Mora, L. de, Kuhlbrodt, T., Rumbold, S., Kelley, D. I., Ellis, R., Johnson, C. E., Walton, J., Abraham, N. L., Andrews, M. B., Andrews, T., Archibald, A. T., Berthou, S., Burke, E., Blockley, E., Carslaw, K., Dalvi, M., Edwards, J., Folberth, G. A., Gedney, N., Griffiths, P. T., Harper, A. B., Hendry, M. A., Hewitt, A. J., Johnson, B., Jones, A., Jones, C. D., Keeble, J., Liddicoat, S., Morgenstern, O., Parker, R. J., Predoi, V., Robertson, E., Siahahan, A., Smith, R. S., Swaminathan, R., Woodhouse, M. T., Zeng, G. and Zerroukat, M.: UKESM1: Description and evaluation of the UK Earth
610 System Model, *Journal of Advances in Modeling Earth Systems*, n/a(n/a), doi:10.1029/2019MS001739, 2020.
- Shao, P., Zeng, X., Sakaguchi, K., Monson, R. K. and Zeng, X.: Terrestrial Carbon Cycle: Climate Relations in Eight CMIP5 Earth System Models, *J. Climate*, 26(22), 8744–8764, doi:10.1175/JCLI-D-12-00831.1, 2013.
- Shi, M., Fisher, J. B., Brzostek, E. R. and Phillips, R. P.: Carbon cost of plant nitrogen acquisition: global carbon cycle impact from an improved plant nitrogen cycle in the Community Land Model, *Global Change Biology*, 22(3), 1299–1314,
615 doi:10.1111/gcb.13131, 2016.
- Smith, B., Wårlind, D., Arneth, A., Hickler, T., Leadley, P., Siltberg, J. and Zaehle, S.: Implications of incorporating N cycling and N limitations on primary production in an individual-based dynamic vegetation model, *Biogeosciences*, 11(7), 2027–2054, doi:https://doi.org/10.5194/bg-11-2027-2014, 2014.
- Song, J., Wan, S., Piao, S., Knapp, A. K., Classen, A. T., Vicca, S., Ciais, P., Hovenden, M. J., Leuzinger, S., Beier, C.,
620 Kardol, P., Xia, J., Liu, Q., Ru, J., Zhou, Z., Luo, Y., Guo, D., Adam Langley, J., Zscheischler, J., Dukes, J. S., Tang, J.,

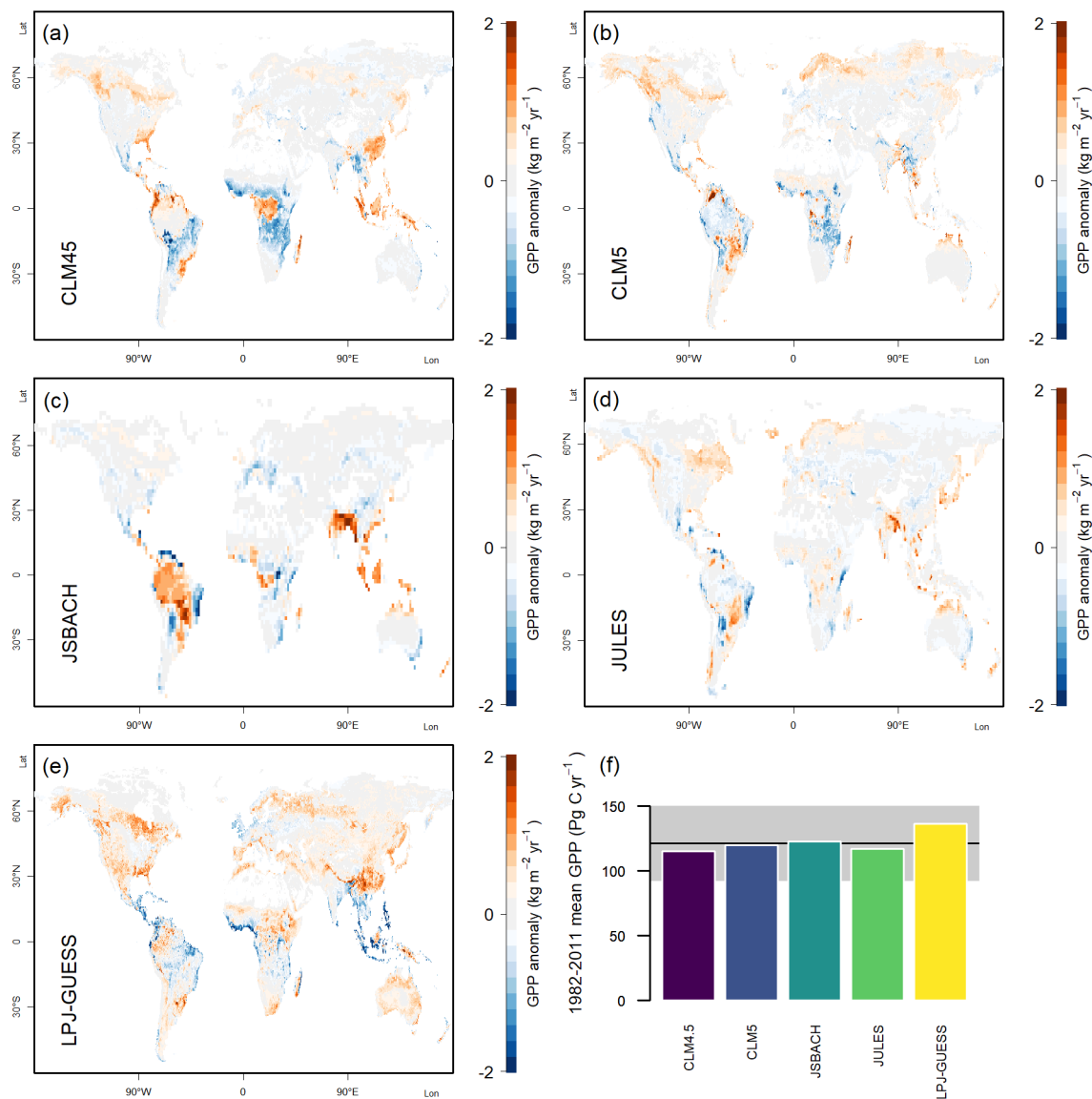


- Chen, J., Hofmockel, K. S., Kueppers, L. M., Rustad, L., Liu, L., Smith, M. D., Templer, P. H., Quinn Thomas, R., Norby, R. J., Phillips, R. P., Niu, S., Fatichi, S., Wang, Y., Shao, P., Han, H., Wang, D., Lei, L., Wang, J., Li, X., Zhang, Q., Li, X., Su, F., Liu, B., Yang, F., Ma, G., Li, G., Liu, Y., Liu, Y., Yang, Z., Zhang, K., Miao, Y., Hu, M., Yan, C., Zhang, A., Zhong, M., Hui, Y., Li, Y. and Zheng, M.: A meta-analysis of 1,119 manipulative experiments on terrestrial carbon-cycling responses to global change, *Nature Ecology & Evolution*, 3(9), 1309–1320, doi:10.1038/s41559-019-0958-3, 2019.
- 625 Taylor, K. E., Stouffer, R. J. and Meehl, G. A.: An Overview of CMIP5 and the Experiment Design, *Bulletin of the American Meteorological Society*, 93(4), 485–498, doi:10.1175/BAMS-D-11-00094.1, 2012.
- Thornton, P. E., Doney, S. C., Lindsay, K., Moore, J. K., Mahowald, N., Randerson, J. T., Fung, I., Lamarque, J.-F., Feddes, J. J. and Lee, Y.-H.: Carbon-nitrogen interactions regulate climate-carbon cycle feedbacks: results from an atmosphere-ocean general circulation model, *Biogeosciences*, 6(10), 2099–2120, doi:https://doi.org/10.5194/bg-6-2099-2009, 2009.
- 630 Walker, A. P., Zaehle, S., Medlyn, B. E., Kauwe, M. G. D., Asao, S., Hickler, T., Parton, W., Ricciuto, D. M., Wang, Y.-P., Wårlind, D. and Norby, R. J.: Predicting long-term carbon sequestration in response to CO₂ enrichment: How and why do current ecosystem models differ?, *Global Biogeochemical Cycles*, 29(4), 476–495, doi:10.1002/2014GB004995, 2015.
- 635 Weedon, G. P., Gomes, S., Viterbo, P., Shuttleworth, W. J., Blyth, E., Österle, H., Adam, J. C., Bellouin, N., Boucher, O. and Best, M.: Creation of the WATCH Forcing Data and Its Use to Assess Global and Regional Reference Crop Evaporation over Land during the Twentieth Century, *J. Hydrometeorol.*, 12(5), 823–848, doi:10.1175/2011JHM1369.1, 2011.
- Wieder, W. R., Cleveland, C. C., Lawrence, D. M. and Bonan, G. B.: Effects of model structural uncertainty on carbon cycle projections: biological nitrogen fixation as a case study, *Environ. Res. Lett.*, 10(4), 044016, doi:10.1088/1748-9326/10/4/044016, 2015a.
- 640 Wieder, W. R., Cleveland, C. C., Smith, W. K. and Todd-Brown, K.: Future productivity and carbon storage limited by terrestrial nutrient availability, *Nature Geoscience*, 8(6), 441–444, doi:10.1038/ngeo2413, 2015b.
- Wieder, W. R., Lawrence, D. M., Fisher, R. A., Bonan, G. B., Cheng, S. J., Goodale, C. L., Grandy, A. S., Koven, C. D., Lombardozzi, D. L., Oleson, K. W. and Thomas, R. Q.: Beyond Static Benchmarking: Using Experimental Manipulations to Evaluate Land Model Assumptions, *Global Biogeochemical Cycles*, 33(10), 1289–1309, doi:10.1029/2018GB006141, 2019.
- 645 Zaehle, S. and Dalmonech, D.: Carbon–nitrogen interactions on land at global scales: current understanding in modelling climate biosphere feedbacks, *Current Opinion in Environmental Sustainability*, 3(5), 311–320, doi:10.1016/j.cosust.2011.08.008, 2011.
- Zaehle, S., Medlyn, B. E., De Kauwe, M. G., Walker, A. P., Dietze, M. C., Hickler, T., Luo, Y., Wang, Y.-P., El-Masri, B., Thornton, P., Jain, A., Wang, S., Warlind, D., Weng, E., Parton, W., Iversen, C. M., Gallet-Budynek, A., McCarthy, H., Finzi, A., Hanson, P. J., Prentice, I. C., Oren, R. and Norby, R. J.: Evaluation of 11 terrestrial carbon–nitrogen cycle models against observations from two temperate Free-Air CO₂ Enrichment studies, *New Phytol.*, 202(3), 803–822, doi:10.1111/nph.12697, 2014a.
- 650

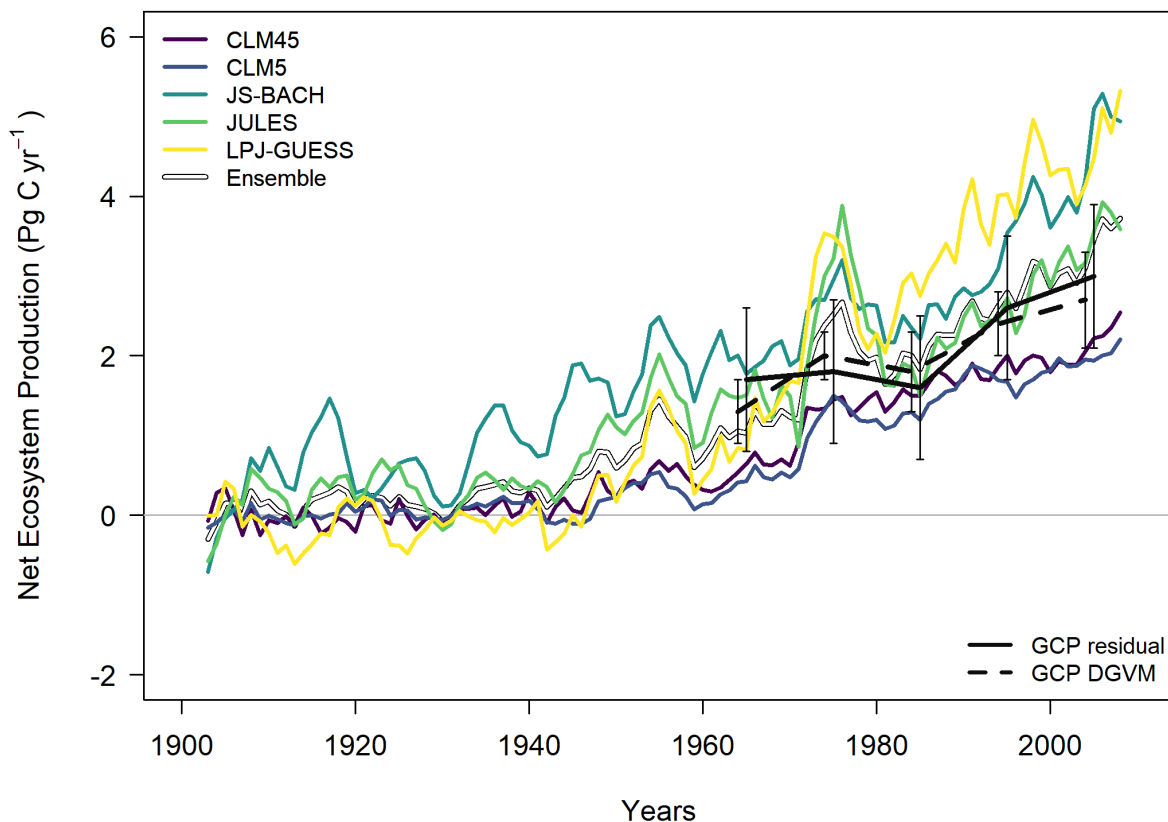


655 Zaehle, S., Jones, C. D., Houlton, B., Lamarque, J.-F. and Robertson, E.: Nitrogen Availability Reduces CMIP5 Projections
of Twenty-First-Century Land Carbon Uptake, *J. Climate*, 28(6), 2494–2511, doi:10.1175/JCLI-D-13-00776.1, 2014b.
Zak, D. R., Freedman, Z. B., Upchurch, R. A., Steffens, M. and Kögel-Knabner, I.: Anthropogenic N deposition increases
soil organic matter accumulation without altering its biochemical composition, *Global Change Biology*, 23(2), 933–944,
doi:10.1111/gcb.13480, 2017.

660

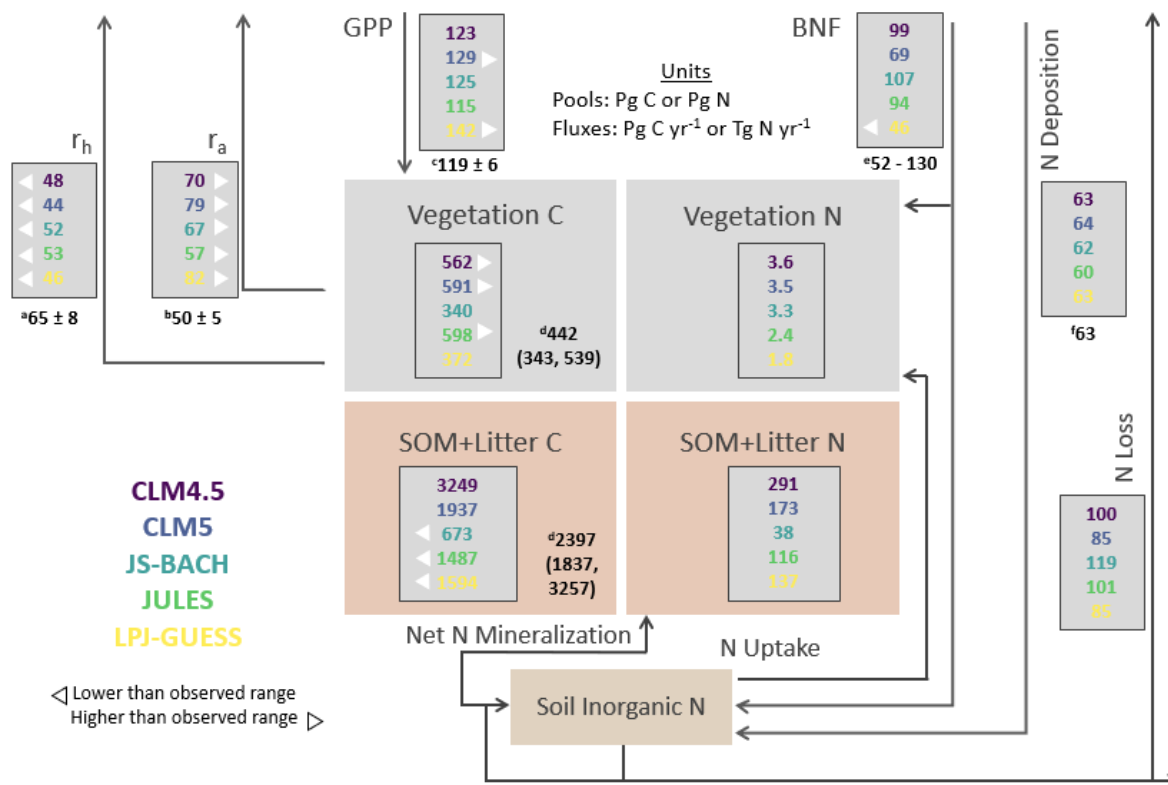


665 **Figure 1. Model output of 1982-2011 mean gross primary productivity (GPP). (a) – (e) Model estimates, shown as anomaly of the corresponding observation-based estimate (MTE) published by Jung et al. (2011). (f) Globally integrated estimates. Black line indicates the global average from the observation-based source; grey area indicates the globally integrated standard deviation from the global average in the model tree ensemble applied to obtain the global average.**

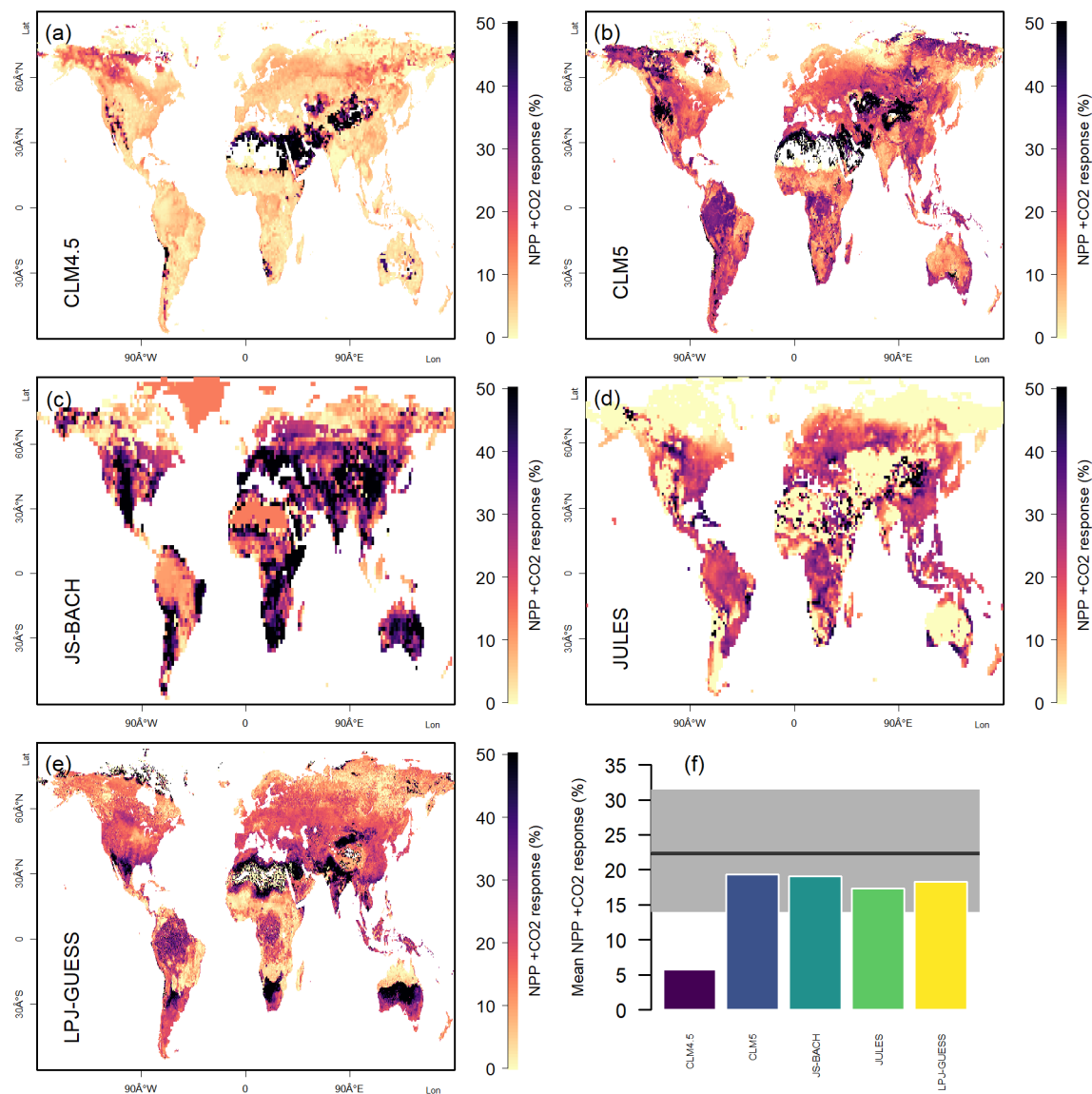


670 **Figure 2. Model predictions (five year moving averages) of 1901-2010 global net ecosystem production (NEP). Coloured curves**
show model predictions as anomalies to the 1901-1910 mean, “Ensemble” shows the model average. Black curves and error bars
indicate assessments published by the Global Carbon Project (Friedlingstein et al., 2019). “GCP residual” shows the estimates and
uncertainty resulting from the consideration of all constituting global fluxes as a “residual sink”. “GCP DGVM” shows the
combined estimate ± 1 standard deviation from an ensemble of global vegetation models.

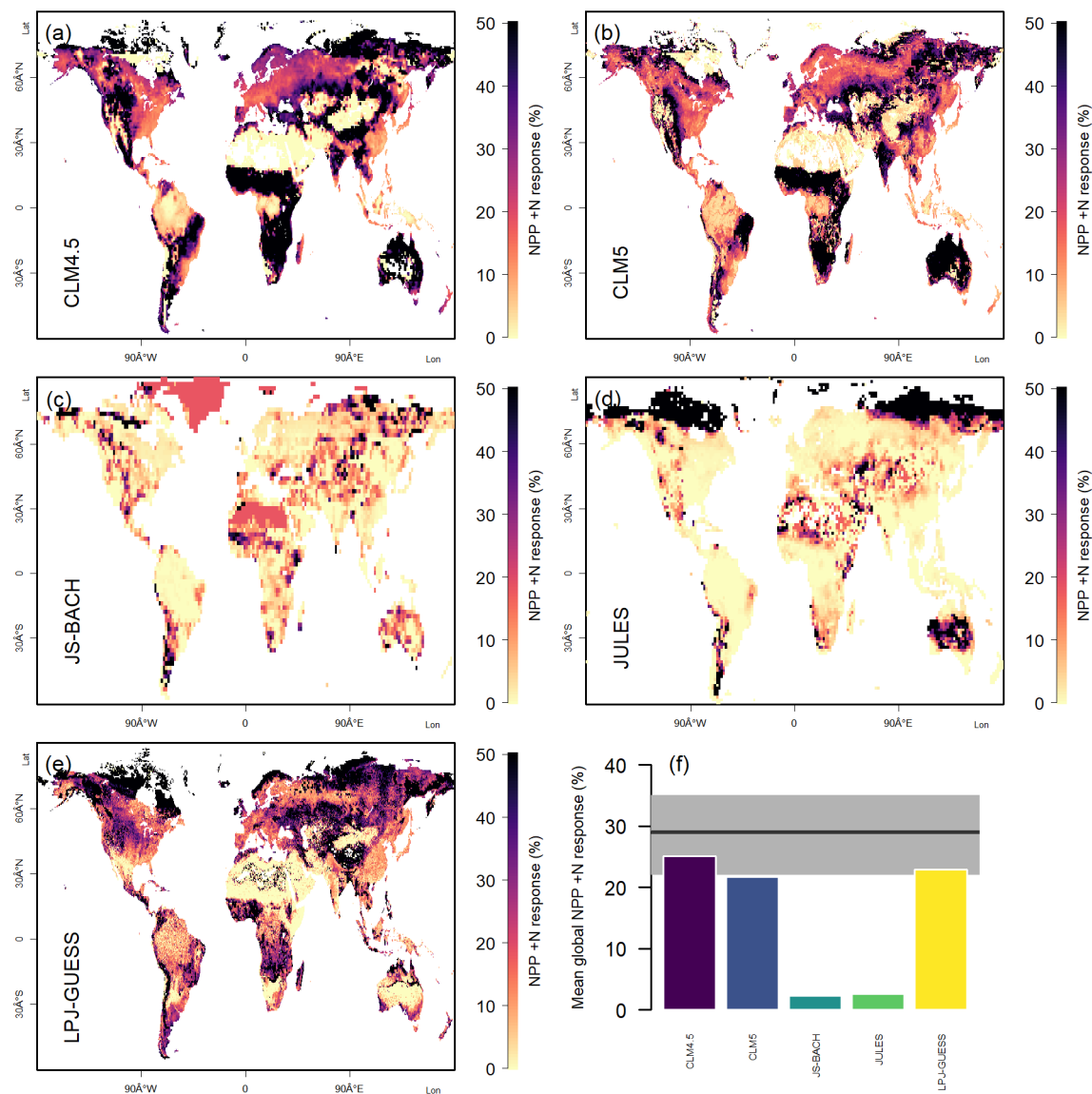
675



680 Figure 3. 1996-2005 mean model estimates of the major ecosystem C and N component pools and fluxes in comparison with
 observation-based estimates from the literature. C = Carbon; N = Nitrogen; r_h = Heterotrophic respiration; r_a = Autotrophic
 respiration; GPP = Gross primary productivity; SOM = Soil organic matter; BNF = Biological nitrogen fixation; The N uptake
 flux refers to root uptake of inorganic N. N loss is the loss via gaseous loss and leaching. The black numbers indicate observation-
 based estimates from the literature: a) Heterotrophic respiration: Bond-Lamberty & Thomson (2010), soil respiration estimate for
 2008. To account for the included root respiration, we reduced the literature estimate by 33% according to Bowden et al. (1993);
 685 b) Autotrophic respiration: Piao et al. (2010), Luyssaert et al. (2007), present day estimate for forests from 2007; c) GPP: Jung et
 al. (2011), averaged estimate for 1982-2011; d) SOM+Litter: Carvalhais et al. (2014), present day estimate from 2014; e) BNF:
 Davies-Barnard and Friedlingstein, (forthcoming) global total BNF; f) N deposition: Lamarque et al. (2010), estimate for 2000.



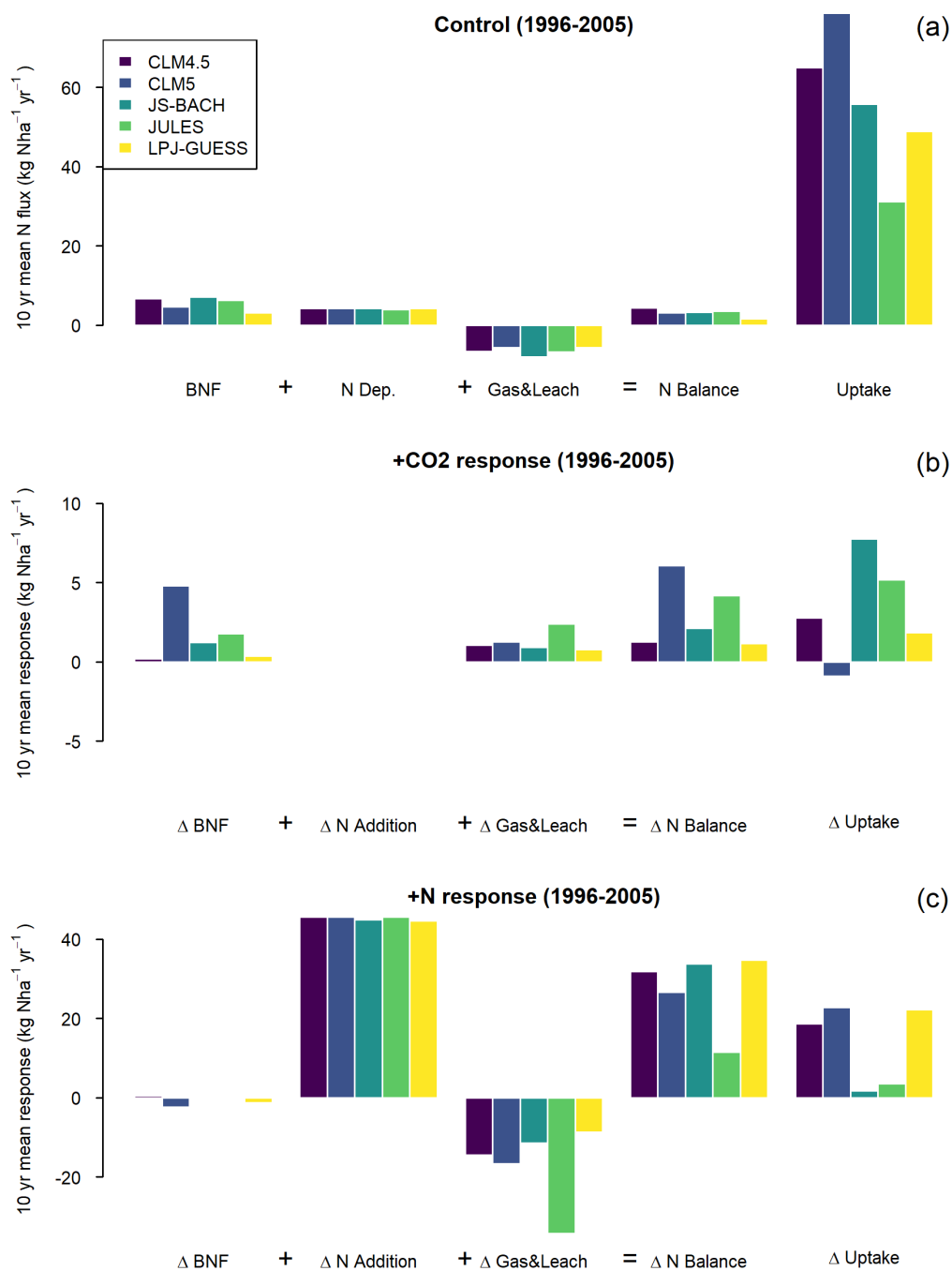
690 **Figure 4.** Model estimates of 1996-2005 mean net primary productivity (NPP) response to +CO₂. (a) – (e) Model estimates, shown as the anomaly compared to the model control scenario. Values above 50% are given the 50% colour. (f) Globally integrated estimates. Black line indicates the global average observed NPP responses to +CO₂ (Baig et al., 2015); grey area indicates the uncertainty range from the observations.



695

Figure 5. Model estimates of 1996-2005 mean net primary productivity (NPP) response to +N. (a) – (e) Model estimates, shown as the anomaly compared to the model control scenario. Values above 50% are given the 50% colour. (f) Globally integrated estimates. Black line indicates the global average observed NPP responses to +N (LeBauer and Treseder, 2008); grey area indicates the uncertainty range from the observations.

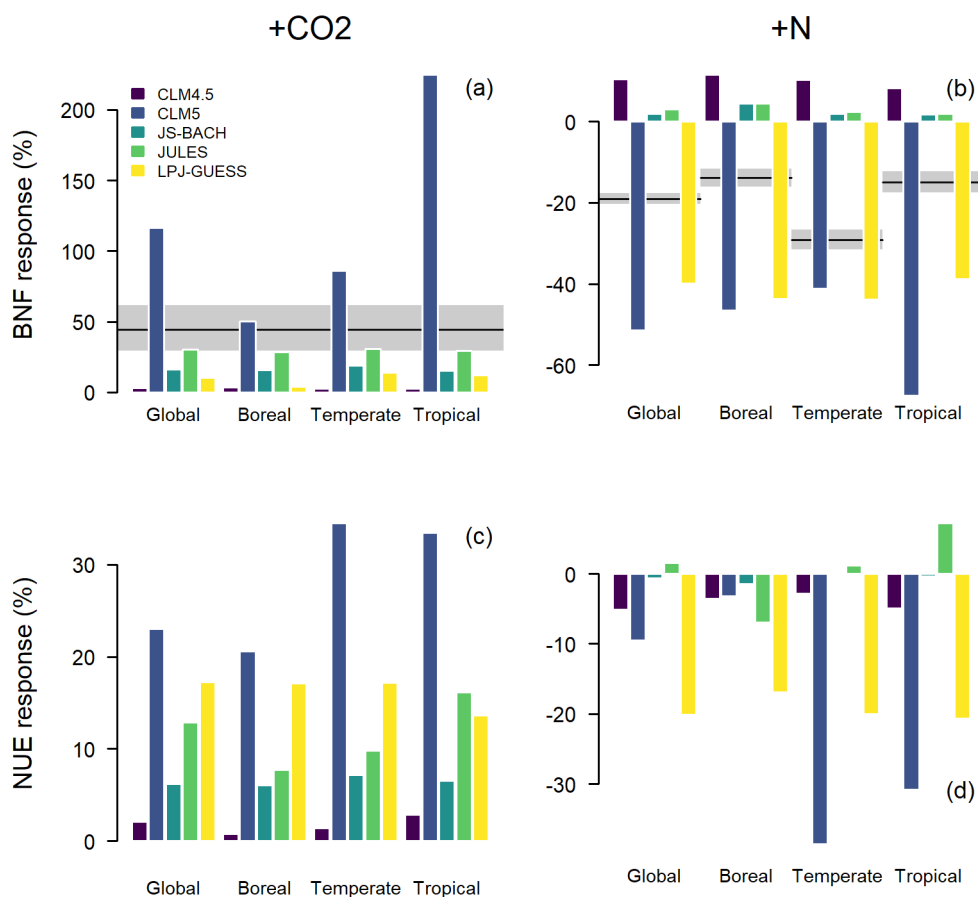
700



705 **Figure 6.** Global averaged 1996-2005 biological nitrogen fixation (BNF), N deposition, N loss via gaseous and leaching, the balance of those three inputs/losses, and the N uptake of the models. The top panel represents the Control scenario, and the second and third panels the response to +CO₂ and +N perturbations (Methods). Note that the y-axis scale is 4x smaller for +CO₂ response than the Control or +N response.

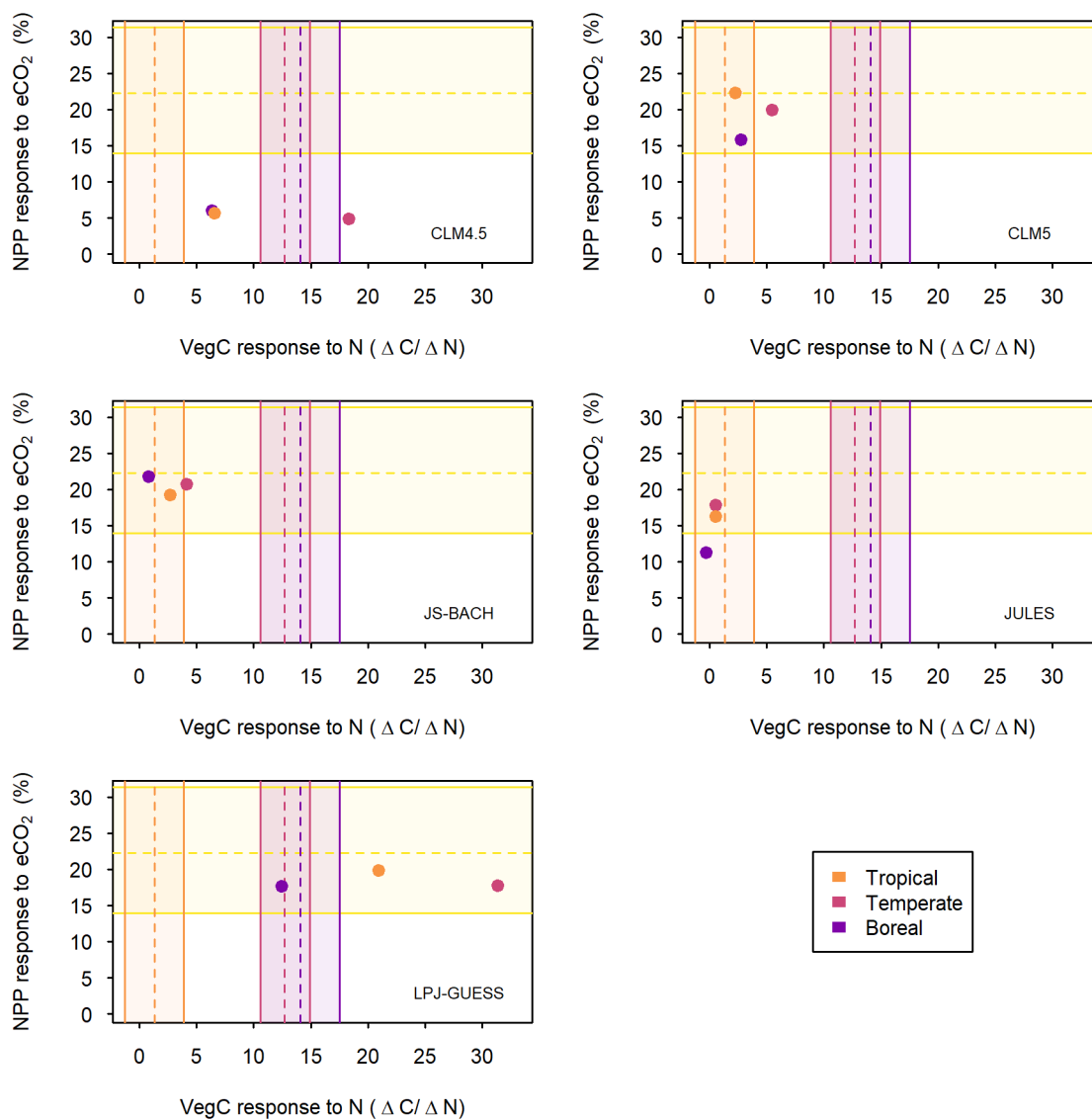


710



715

Figure 7. Averaged 1996-2005 responses in biological nitrogen fixation (BNF) and nitrogen-use efficiency (NUE; see Eq. 1) to +CO₂ and +N perturbations (Methods). (a) Model BNF responses to +CO₂. Black line and grey area indicate mean and 95% CI of the global estimate published by Liang et al. (2016). (b) Model BNF responses to +N. Black lines and grey areas indicate means and 95% confidence intervals of the estimates published by Zheng et al. (2019). (c) Model NUE responses to +CO₂. (d) Model NUE responses to +N. Biomes according to Köppen-Geiger climate classification (Kottek et al., 2006).



720

Figure 8. Average 1996-2005 model predictions of net primary productivity (NPP) responses to +CO₂ (y-axis) and aboveground vegetation carbon (C) pool size responses to nitrogen (N) addition (x-axis) for each of the models (as labelled). Area outlined in yellow indicates synthesis of observed NPP responses to +CO₂ (Baig et al., 2015). Other coloured areas indicate biome-wise estimates of aboveground forest C change per added N (Schulte-Uebbing et al., 2018). Model results restricted to simulated vegetation with NPP > 0.2 kg C m⁻² yr⁻¹. Biomes according to Köppen-Geiger climate classification (Kottek et al., 2006).

725

730



	CLM4.5	CLM5	JSBACH	JULES	LPJ-GUESS
Key references	Oleson et al. (2013)	Lawrence et al. (2020)	Goll, et al. (2017), Mauritsen et al. (2019)	Wiltshire et al. (forthcoming)	Smith et al. (2014)
N effect on GPP	Downregulation of GPP to match stoichiometric constraint from allocable N	Leaf N compartmentalized into different pools to co-regulate photosynthesis according to the LUNA model	No direct effect	No direct effect	Reduction of rubisco capacity in case of N stress
N effect on autotrophic respiration	N content-dependent tissue-level maintenance respiration	Updated PFT-specific N-dependent leaf respiration scheme	No direct effect	N content-dependent maintenance respiration for roots and stems	N content-dependent maintenance respiration for roots and stems; leaf respiration reduced under N stress
Vegetation pool C:N stoichiometry	Fixed for all pools	Flexible for all pools	Fixed for all pools except labile	Flexible leaf stoichiometry from which root and stem C:N are scaled with fixed fractions	Flexible for leaves and fine roots, fixed otherwise
Retranslocation of N from shed leaves	Fraction of leaf N moved to mobile plant N pool prior to shedding. Fraction depends on PFT-specific fixed live leaf and leaf litter C:N ratios.	Fraction of leaf N moved to mobile plant N prior to shedding via two pathways: a free retranslocation, or a paid-for retranslocation dependent on PFT-specific dynamic leaf C:N range and minimum leaf litter	Fraction of leaf N moved to mobile plant N pool prior to shedding	Fraction of leaf N moved to labile store with PFT specific retranslocation coefficient	Fraction of leaf N moved to mobile plant N pool prior to shedding. Fraction depends on N stress.



		C:N and available carbon to spend for extraction in FUN model				
Biological fixation	N	Monotonically increasing function of NPP	Symbiotic N fixation according to the FUN model, asymbiotic N fixation linearly dependent on evapotranspiration	Non-linear function of NPP	Linear function of NPP, 0.0016 kg N per kg C NPP	Linear function of ecosystem evapotranspiration, 0.102 cm yr ⁻¹ ET +0.524 per kg N ha ⁻¹
Ecosystem loss	N	Denitrification loss as fraction of gross N mineralization + fraction of soil inorganic N pool in case of N saturation (CLM-CN) / Denitrification as fraction of nitrification (CENTURY) Leaching as function of soil inorganic N pool size Fractional fire loss as fraction of vegetation and litter pools	Denitrification as fraction of nitrification (CENTURY) Leaching as function of soil inorganic N pool size Fractional fire loss as fraction of vegetation and litter pools	Denitrification proportional to soil inorganic N pool and soil moisture Leaching proportional to soil inorganic N pool and drainage	Denitrification is a fixed fraction (1%) of mineralization flux Leaching of nitrogen is a function of soil inorganic N pool, drainage, and a parameter representing the effective solubility of nitrogen	Denitrification as fixed fraction of mineralization flux Leaching as function of soil inorganic N pool and drainage N loss from fire events
Plant N uptake		Function of plant N demand, soil inorganic N availability, and competition with heterotrophs	Soil uptake of inorganic N according to the FUN model	Plant N demand-based, limited by soil inorganic N availability	Demand based on GPP and limited by soil inorganic N availability	Determined to maintain optimal leaf N for photosynthesis, limited by soil inorganic N availability, fine root mass, soil temperature



					and plant N status
--	--	--	--	--	--------------------

Table 1. Key nitrogen cycle algorithms applied by the models. C = Carbon; N = Nitrogen; GPP = gross primary productivity; NPP = net primary productivity; PFT = plant functional type